Table 9

Quantifying human influence on drought and drought termination characteristics in disturbed period.

Case study	Predominant human activity	Changes in drought characteristics (%)				Changes in drought termination characteristics (%)		
		Drought frequency (D_{freq})	Mean drought duration (D_{dur})	Mean drought deficit (D_{def})	Mean maximum intensity (MI)	Mean termination duration (DT_{dur})	Mean termination deficit (DT_{def})	Mean termination rate (DT_{rate})
Xiquan	——	+3	–4	–3	–3	–5	–3	–2
Xiaochengzi	Human water withdrawal	–63	**+601**	**+1376**	**+209**	**+230**	**+865**	**+35**
Dianzi	Reservoir regulations, Human water withdrawal	+29	+121	+208	+106	+73	+170	+26
Taipingzhuang	Land use change, Human water withdrawal	–15	+248	+619	+128	+192	+404	+21

An approach for identification and quantification of hydrological drought termination characteristics of natural and human-influenced series

Menghao Wang[a, b], Shanhu Jiang[a, b]*, Liliang Ren[a, b], Chong-Yu Xu[c], Fei Yuan[a, b], Yi Liu[b], Xiaoli Yang[b]

[a]State Key Laboratory of Hydrology-Water Resources and Hydraulic Engineering, Hohai University, Nanjing 210098, China

[b]College of Hydrology and Water Resources, Hohai University, Nanjing 210098, China

[c]Department of Geosciences, University of Oslo, Oslo, Norway

Submitted to *Journal of Hydrology*

*Corresponding author:

Professor Shanhu Jiang

State Key Laboratory of Hydrology-Water Resources and Hydraulic Engineering, Hohai University, Nanjing 210098, China

Email: hik0216@hhu.edu.cn

Abstract

Although many previous studies have analysed the impacts of human activities on hydrological drought, studies that analysed these impacts from the perspective of drought termination, a critical re-wetting phase of hydrological drought, are limited. A deeper understanding on how human alter hydrological drought termination phase is essential for improving drought recovery prediction and performance of the drought early warning system. In this study, a comprehensive approach for identifying hydrological drought termination characteristics and quantifying the impact of human activities on drought termination was proposed. This approach, which combines the concept of drought termination (DT), an 'observed–simulated' comparison approach, and the variable threshold level method (TLM_v), consists of the following steps: (1) reconstruction of natural streamflow using a hydrological model, (2) identification of hydrological drought termination characteristics using TLM_v method and the concept of drought termination, and (3) quantification of human influence by comparison of the hydrological drought termination characteristics of human-influenced (observed) series and those of natural (simulated) series. The Laohahe basin, consists of four catchments (Xiquan, Xiaochengzi, Dianzi, and Taipingzhuang) in northern China, was evaluated using the proposed procedure. The study demonstrated that the proposed approach is efficient in quantifying human influence on hydrological drought termination phase. The results revealed that human activities have significant impacts on the hydrological drought termination phase in the Xiaochengzi, Dianzi, and

Taipingzhuang catchments. All the average drought termination duration (DT_{dur}), deficit (DT_{def}), and rate (DT_{rate}) in the human-influenced series of the three catchments (Xiaochengzi, Dianzi, and Taipingzhuang) increased in comparison to those in the natural series, with maximum increases of 230%, 865%, and 35%, respectively. The seasonality of the drought termination phase starts (DT_{start}) and ends (DT_{end}) for the three catchments exhibited obvious shifts due to human influence. The preferred seasons for DT_{start} and DT_{end} were shifted to summer and autumn, respectively. The proposed approach and findings of this study may help to gain a deeper understanding of how human activities alter hydrological drought termination severity (drought termination duration, deficit, and rate) and time (drought termination starts or ends).

Keywords: Hydrological drought; Human activities; Drought termination; Variable threshold level method

1. Introduction

Drought is recognised as a natural disaster and occurs in most parts of the world, even in wet and humid regions (Forzieri et al., 2014; Van Lanen et al., 2013; Sheffield et al., 2012; Dai, 2011; Mishra and Singh, 2010; Fleig et al., 2006; Li et al., 2020a,b; Jiang et al., 2020). Dry periods lasting from years to decades occurred many times in regions all over the world during the last millennium, and global aridity has increased substantially since the 1970s (Dai, 2011; Zargar, 2011; Krysanova et al., 2008; Palmer et al., 2008; Sheffield, 2012; Watts et al., 2012). Because of the increasing demand for water stimulated by population growth and expansion of the agricultural, energy and industrial sectors, drought events have attracted the attention of environmentalists, ecologists, hydrologists, meteorologists, geologists, and agricultural scientists (Mishra and Singh, 2010; Van Loon, 2015; Lettenmaier and Gan, 1990; Andreadis et al., 2006). According to different types of water deficits, droughts are commonly classified into four types: meteorological drought, hydrological drought, agricultural drought, and socioeconomic drought (Ma et al., 2014; Mishra and Singh, 2010; Jiang et al., 2019; Dehghani and Zargar, 2019; Yeh, 2019; Chen et al., 2019).

Hydrological drought, which is manifested by abnormally low streamflow in rivers and abnormally low levels in lakes, reservoirs, or/and groundwater (Tallaksen and Van Lanen, 2004; Van Loon and Van Lanen, 2013), is susceptible to human activities (Ahmadi et al., 2019; Xia et al., 2019). Many studies have analysed how different human influences (e.g., human water withdrawal, reservoir regulations, and land cover change) affect hydrological drought process (Jiang et al., 2019; Wu et al., 2019; Yuan et al., 2018; Van Loon and Van Lanen, 2013; Lin et al., 2017; Zou et al., 2018).

However, a critical re-wetting phase of hydrological drought, termed hydrological drought termination, has been relatively neglected (Parry et al., 2016). Lack of knowledge of this process hinders water managers to decide how the transition from depleted to replenished water supplies is operationally handled (Hannaford et al., 2011; Bell et al., 2013). Therefore, the focus of this study is to explore how hydrological drought termination phase (including duration, deficit, rate, and time at which drought termination start or end) changes under human influence, which is crucial for improving the forecasting of drought recovery and establishing a reliable drought monitor system.

Just like drought defined in many different ways, different drought assessment methods or indices based on one or more variables (e.g., precipitation, streamflow, or soil moisture) also have their own drought termination criteria (Heim Jr. and Brewer, 2012; Parry et al., 2016). The earliest researches assessed drought termination according to climatological probability (Byun and Wilhite, 1999), applying indices such as the Palmer Drought Severity Index (PDSI) and the Standardised Precipitation Index (SPI). Since then, many methods or indices were proposed to calculate the amount of rainfall required to terminate a drought under given meteorological inputs (Bell et al., 2013; Pan et al., 2013; Antofie et al., 2014; Parry et al., 2018). These studies focus on meteorological or soil moisture drought termination, whereas there is a need to address hydrological drought termination more holistically (Margariti et al., 2019). Parry et al. (2016) pointed out that a number of studies have attempted to characterize the drought termination phase and reviewed a number of questions and knowledge gaps regarding drought termination that remain unanswered. And then, they proposed a definition of drought termination, and applied this new concept to a case study of the 2010–2012 drought in the UK, and the propagation of drought termination between river flows and groundwater levels. In this study, we followed the definition proposed by Parry et al. (2016), who defined drought termination as a period between the maximum negative anomaly and a return to above-average conditions. It is not only a point in time describing when a drought is said to have ended but also a quantifiable event with a temporal profile. Once this phase has been delineated, the duration, deficit, rate and seasonality of hydrological drought termination can be derived.

Threshold level method (TLM) (Van Loon and Van Lanen, 2013; Sarailidis et al., 2019; Jiang et al., 2019) is a commonly used method for extracting propagation characteristics of hydrological drought (e.g. drought duration and deficit) and drought termination (e.g. drought termination duration and deficit). The threshold level method (TLM), proposed by Yevjevich (1967), considers a hydrological drought events to occur when the variable of interest (e.g., streamflow or groundwater level) falls below a predefined threshold. When this method is applied to quantify the impact of human activities, the threshold values are usually calculated based on the full length of naturalised (simulated) streamflow and then are used to identify drought events in both natural series and human-influenced series. Differences between the two series reflect human influence on hydrological drought and drought termination.

Many comparative analysis methods (Van Loon et al., 2019; Wu et al., 2019) have been used to quantify the impact of human activities on hydrological drought.

Van Loon et al. (2019) proposed the 'paired basin comparative' approach and selected two different basins to represent disturbed and undisturbed situations. However, it is usually difficult to find two watersheds that have similar physical characteristics other than specific human influences. The 'upstream–downstream' approach, introduced by Rangecroft et al. (2019), used observation data only, including disturbed downstream and undisturbed upstream portions, to analyse human influence. The 'pre–post-disturbance comparative' approach (Liu et al., 2016; Rangecroft et al., 2019) is usually employed to assess the impact of reservoirs on hydrological drought. However, these two comparative analysis methods are always limited to the analysis of specific human influence. Compared with the above methods, the 'observed–simulated comparison' method has more modest data requirements, including meteorological forcing as input and hydrological data of the 'undisturbed period' for calibration (Van Loon and Van Lanen, 2013). This is the first advantage of this method. In addition, many basins are affected by complex and diverse human activities, and naturalised data (e.g., reservoir regulation records, human water withdrawal records) are often sensitive or unreliable. Application of different methods of data naturalisation to different basins also introduces uncertainty into cross-basin comparisons. The 'observed–simulated' comparison method uses hydrological models to simulate near-natural hydrological variables for different basins and compares these variables with those of observed series to avoid the above uncertainties. This is another advantage of this method. Based on these advantages of this comparison method and its successful applications, 'observed-simulated' comparative approach was used in our study. Nowadays, an increasing number of hydrological models have been used to quantify human influences on hydrological drought, including the Variable Infiltration Capacity (VIC) (Liu et al., 2016; Jiang et al., 2019), the Soil Water and Assessment Tool (SWAT) (Wu et al., 2019), and the HBV (Van Loon and Van Lanen, 2013) model.

A few recent good studies have focused on human influence to hydrological drought termination phase. Margariti et al. (2019) assessed if and how human modifications affect the drought termination phase by considering the human activities of reservoirs, abstraction, urbanisation and water transfer. Wu et al. (2019) used the Standardized Streamflow Index to assess the impact of human regulations on hydrological drought development and recovery based on a 'simulated–observed' comparison. However, these studies either used different approaches to reconstruct natural streamflow (which may introduce some inconsistency into cross-catchment comparisons), or did not consider the start and/or end time characteristic of hydrological drought termination phase. Therefore, a comprehensive assessment considering the reconstruction of natural streamflow, identification of hydrological drought termination characteristics, and quantification of human influence on hydrological drought termination phase is valuable to understand how human activities alter hydrological drought termination phase, especially in this "human-influenced era" (Van Loon et al., 2016).

This study proposed a comprehensive assessment approach for identifying and quantifying drought termination characteristics of natural series and human-influenced series, which consist of three steps: (1) using a hydrological model to reconstruct the natural streamflow of human-influenced regions; (2) extracting hydrological drought events using the variable threshold level method and identify hydrological termination characteristics through the concept of drought termination; and (3) quantifying impact of human activities on hydrological drought termination using the 'simulated-observed' comparison method. The proposed approach differs from previous studies with the following features: (1) to maintain consistency and uniformity in the reconstructed natural streamflow between the catchments, the same hydrological model was used for flow simulation in all four catchments, (2) special attention was paid to low flows in model calibration and simulation, (3) to ensure reliability and validity of the reconstructed natural streamflow, we used a 'nature catchment' (relatively not influenced by human activities) to validate the model, and (4) the proposed approach can identify both drought termination severity characteristics (e.g. drought termination duration, deficit, and rate) and drought termination time characteristics (e.g. seasons when the drought termination phase starts and/or ends). The Laohahe basin in northern China, was chosen to perform the study because its quantity of available water resources has decreased significantly and hydrological drought within the basin has occurred frequently under intense human influence (Yong et al., 2013; Jiang et al., 2011; Liu et al., 2009). The results of this study will be helpful for formulating appropriate responses to drought conditions and improving the effectiveness of local drought monitor.

2. Study area and data

2.1. Study area

2.1.1. The Laohahe basin

The Laohahe basin is located at the junction of the Hebei and Liaoning provinces and the Inner Mongolia Autonomous Region in north-eastern China (118°15′−120°E, 41°−42°15′N) (Fig. 1). It covers an area of 7,720 km^2, with the Taipingzhuang hydrological station (42°12′N, 119°15′E) at the basin outlet (Liu et al., 2009). The elevation within the basin ranges from 478 m to 1808 m above mean sea level, decreasing from the southwest to the northeast (Yong et al., 2013). Because of the uneven spatial and temporal distribution of precipitation (approximately 88% of the annual precipitation occurs from May to September), streamflow of the Laohahe basin exhibits strong seasonality (Jiang et al., 2012).

In this study, four catchments of the Laohahe basin (Fig. 1) were selected, including Xiquan, Xiaochengzi, Dianzi, and Taipingzhuang catchments. The geographic and hydrological characteristics of these catchments are listed in Table 1. The range of average annual precipitation of these catchments is 438−573 mm, and the range of average annual streamflow is 26–127 mm. Spatial variation of precipitation caused both precipitation and streamflow of the basin decrease gradually from the southwest to the northeast.

2.1.2. Human activities in the Laohahe basin

Previous studies have indicated that there has been a significant decrease in streamflow of the Laohahe basin (Jiang et al., 2019; Liu et al., 2016) as a result of the influence of human activities. Yong et al. (2013) found that change points for both the Taipingzhuang and Dianzi catchments occurred in 1979. Jiang et al. (2011) noted that human activities were the main factors (with contributions of 89–93%) in the streamflow decrease in the basin after 1979. Based on these studies, the Mann–Kendall (M-K) (Mann, 1945; Kendall, 1975) test method was firstly used for the trend analysis of the precipitation, potential evapotranspiration (PET) (calculated via the Penman–Monteith equation recommended by the Food and Agriculture Organization), and streamflow series of the four catchments in the Laohahe basin during the period 1964−2016. The M-K test results (Table 2) showed that there was no significant increasing or decreasing trend in precipitation and PET series for the four catchments, but streamflow series of the Xiaochengzi, Dianzi, and Taipingzhuang catchments (except for the Xiquan catchment) decreased significantly. Then, Pettitt (Pettitt, 1979) test method and the precipitation and streamflow double cumulative curve (DCC) method were used to identify change points of these hydrological variables for the four catchments. The Pettitt test results showed that the first streamflow change points ($1–P > 0.99$) for Xiaochengzi, Dianzi, and Taipingzhuang catchments occurred in 1998, 1979, and 1979, respectively (Table 2). Results of the

DCC method (Fig. 2) also indicated that gradients of the streamflow accumulation curve were significantly different from those of the precipitation accumulation curve for the three catchments after 1998, 1979, and 1979, respectively. And there were no significant change points in precipitation and PET series of the four catchments. Therefore, the Mann-Kendall, Pettitt, and DCC test methods detected that 1998, 1979, 1979 were the streamflow change points for the Xiaochengzi, Dianzi, and Taipingzhuang catchments of the Laohahe basin.

In addition, basic information about the study region, involving population, water utilization, land use changes, and large reservoirs was collected and analysed. Fig. 3 showed land use changes of the study region for different periods (1980, 1990, 2000, 2010, and 2015). Areas of cropland and urban increased significantly and those of forest land, grassland, water, and unused land decreased after 1980. Fig. 4 displayed changes of the socioeconomic data during 1964-2016. It was observed that the population of study region (Fig. 4(a)) was rapidly growing before the 21st century (1964-2000). The GDP (Fig. 4(b)) experienced rapid growth after the national economic opening policy was implemented in 1979. Food production (Fig. 4(c)) and number of livestock (Fig. 4(d)) also experienced rapid growth after 1979. Besides, there is a large reservoir in the study area (Yong et al., 2013), namely the Dahushi (storage capacity: 1.2×10^8 m^3), located in Dianzi catchment. The reservoir started to build in January 1976, completed in October 1979, and began to store water in November 1980. All of these human activities may impact the natural hydrological processes of the basin directly or indirectly, and further influence the hydrological drought and drought termination phase.

2.1.3. Selection of natural catchment for uncertainty analysis of hydrological models

The Xiquan catchment, located at the headwaters of the Laohahe basin, has no significant trend change or change points (Table 2). Besides, it has a consistent relationship between precipitation and streamflow during the entire (undisturbed and disturbed) period (Fig. 2(a)), which means that the streamflow process in this catchment is closed to the natural streamflow process and is little affected by human activities. Thus, the Xiquan catchment was selected as a natural catchment in this study to carry out streamflow simulation and drought assessment together with the other three altered catchments, so as to test the accuracy of the results for the model simulation and drought metrics identification. Here, the calibration (1965-1974) and validation (1975-1979) periods of simulation for Xiquan catchment were as the same as those for the Dianzi and Taipingzhuang catchments.

2.2. Data

The data used in this study consisted of three components: (i) hydrometeorological data, (ii) geographic information data, and (iii) socioeconomic data. The details of the data are as follows.

(1) Daily meteorological forcing data for the period 1964−2016, including the wind speed, maximum and minimum air temperatures measured by six national

standard meteorological stations inside and around the Laohahe basin, were downloaded from the China Meteorological Data Sharing Service System (http://data.cma.cn/). Daily precipitation data measured by 17 rain gauges, daily streamflow records for the four catchments (1964−2016), and information of reservoirs were provided by the Water Resources Department of the Inner Mongolia Autonomous Region. The Inverse Distance Weighting (IDW) method was used to interpolate precipitation and meteorological data into grid data with a resolution of 0.0625° × 0.0625° to drive the VIC hydrological model. For the purpose of comparison with the precipitation data, streamflow data were further converted to runoff (mm) by averaging the runoff amounts (m^3/s) over each catchment area. Because monthly data were used for drought identification in this study, precipitation and streamflow values were further converted from daily to monthly amounts by calculating total monthly values.

(2) The geographic information data included digital elevation model (DEM) data, soil type data, and land use data. The 30-arcsecond global digital elevation model data were obtained from the U.S. Geological Survey (USGS) website (https://www.usgs.gov/). Soil types were derived from the Food and Agriculture Organization (FAO) data set. Land use data were obtained from the University of Maryland's 1-km Global Land Cover Production. All the geographic information data that are needed to drive the VIC model were resampled to a resolution of 0.0625° × 0.0625°.

(3) Socioeconomic data consist of population, gross domestic product (GDP), food production, and number of livestock. Population and GDP data set were provided by Data Centre for Resources and Environmental Sciences, Chinese Academy of Sciences (RESDC) (http://www.resdc.cn). Data of food production and number of livestock were collected from a local statistical bureau website (http://tjj.chifeng.gov.cn/).

3. Methods

This section describes the proposed approach (illustrated in Fig. 5) for identifying hydrological drought termination characteristics and quantifying the impact of human activities on hydrological drought termination. The three main steps in the proposed approach are described below.

The first step focuses on natural streamflow reconstruction. According to the change points identification results, the entire study period can be divided into two periods, namely, the ‘undisturbed period’ (before the change point) and the ‘disturbed period’ (after the change point). The observed hydrological data for the ‘undisturbed period’ were used to calibrate the Variable Infiltration Capacity (VIC) hydrological model, which was selected for use in this study and its detailed description is provided in Section 3.1. And then, the meteorological forcing data for the ‘disturbed period’ were used as input data to the calibrated model to reconstruct (simulate) the natural streamflow during the same period. We considered the simulated streamflow during the ‘disturbed period’ to be the natural streamflow, which is only affected by climate factors. Difference between natural and observed streamflow therefore should be attributed to human activities.

The second step is to identify hydrological drought termination characteristics. The monthly variable threshold level method (TLM_v) was selected as the identification method for hydrological drought events. And then, concept of drought termination was used to extract drought termination metrics, including the drought termination duration, deficit, rate, and the seasons at which drought termination starts or ends.

In the final step, the impacts of human activities on hydrological drought termination (i.e., changes in percentage terms) were quantified by comparing the characteristics (i.e., DT_{dur}, DT_{def}, and DT_{rate}) of natural series with those of human-influenced (observed) series. The frequencies of the drought termination start and end months (DT_{start} and DT_{end}) for human-influenced and natural series were calculated and summarised in terms of four seasons (spring, summer, autumn, and winter). Shifts in the seasonality of drought termination caused by human influence can be captured by comparing the natural and human-influenced series. Considering the different number of drought events in the two series, the frequency was calculated by converting the number of drought terminations starts or ends in each season to a percentage of the total number of drought events. The concept underlying this approach and the methods used are described in detail in the following sections.

3.1. VIC model

The VIC model (Liang et al., 1994) is a macro-scale semi-distributed hydrological model jointly developed by the University of Washington, the University of California at Berkeley, and Princeton University. The model balances water and surface energy budgets and has been widely used in hydrological process simulation around the world (Liang et al., 2004; Adam et al., 2007; Pan et al., 2008). Daily-scale or shorter-time-scale meteorological forcing data (e.g., precipitation, air temperature, wind speed, radiation, etc.) are often used as inputs to simulate land surface hydrological processes (e.g., streamflow, moisture storage, evaporation, etc.) over corresponding time scales.

According to previous studies, the model parameters can be classified into two categories (Liang et al., 2004). The first category consists of parameters that have clear physical meanings and can be determined directly from land use data and soil type data, such as the saturated soil potential ψ_s (m), soil porosity θ_s (m^3/m^3), saturated hydraulic conductivity k_s (m/s), and so on. The second category consists of seven conceptual parameters that need to be calibrated. The details of these user-calibrated parameters are listed in Table 3. The maximum sum value of Nash-Sutcliffe efficiency (NSE) and log-transformed NSE (LogNSE) (Merz, et al., 2011; Yuan et al., 2018), coefficient of correlation (CC), and relative error (BIAS), calculated using Eqs. (1) – (5), were used to evaluate the model performance (Jiang et al., 2018). Although NSE is a good metric for hydrological model optimization, it tends to provide high importance to high flows (Yuan et al., 2018). To make sure that the model can capture both high- and low-flow processes, we used the maximum sum of NSE and log-transformed NSE (LogNSE) as the objective function. Because low-flow process is closely related to the onset and development stage of hydrological drought, and high-flow process is often related to termination stage of drought.

$$f = max(NSE) + max(logNSE) \tag{1}$$

$$NSE = 1 - \frac{\sum_{i=1}^{n}\left(Q_{sim}(i) - Q_{obs}(i)\right)^2}{\sum_{i=1}^{n}\left(Q_{obs}(i) - \bar{Q}_{obs}\right)^2} \tag{2}$$

$$logNSE = 1 - \frac{\sum_{i=1}^{n}\left(logQ_{sim}(i) - logQ_{obs}(i)\right)^2}{\sum_{i=1}^{n}\left(logQ_{obs}(i) - log\bar{Q}_{obs}\right)^2} \tag{3}$$

$$CC = \frac{\sum_{i=1}^{n}\left(Q_{obs}(i) - \bar{Q}_{obs}\right)\cdot\left(Q_{sim}(i) - \bar{Q}_{sim}\right)}{\sqrt{\sum_{i=1}^{n}\left(Q_{obs}(i) - \bar{Q}_{obs}\right)^2}\sqrt{\sum_{i=1}^{n}\left(Q_{sim}(i) - \bar{Q}_{sim}\right)^2}} \tag{4}$$

$$BIAS = \frac{\sum_{i=1}^{n}\left(Q_{sim}(i) - Q_{obs}(i)\right)}{\sum_{i=1}^{n}Q_{obs}(i)} \tag{5}$$

Where $Q_{obs}(i)$ and $Q_{sim}(i)$ are the observed and simulated streamflows (mm/month) at time step *i*, $\bar{Q}_{obs}$, $\bar{Q}_{sim}$, and $log\bar{Q}_{obs}$ are the mean observed, simulated , and log-transformed observed streamflow values (mm/month), $logQ_{obs}(i)$ and $logQ_{sim}(i)$ denote the log-transformed observed and simulated streamflows, and *n* is the number of data points.

3.2. Identification of hydrological drought propagation characteristics

3.2.1. The variable threshold level method

In this study, we chose the threshold level method, proposed by Yevjevich (1967), for drought event identification. In this method, a hydrological drought event occurs when the streamflow is below a predefined threshold and continues until the threshold is exceeded again (Tallaksen and Van Lanen, 2004; Pereira et al., 2009; Seneviratne et al., 2012). The selection of the threshold is important, as it can influence the drought characteristics, such as the drought duration (D_{dur}) and deficit volume (D_{def}) (Hisdal et al., 2001; Fleig et al., 2006). Considering the strong seasonal variability of the study basins, the variable threshold level method (TLM_v) was judged to be more appropriate for the purposes of this study than a fixed threshold method. We followed the approach proposed by Van Loon and Van Lanen (2013) to apply monthly thresholds derived from the 70th percentiles of the monthly duration curves. This implies that, for each month, the value of a flux or state variable was chosen, that was equalled or exceeded 70% of the time in that specific month. The variable threshold values were calculated based on the entire (undisturbed period and disturbed period) natural (simulated) streamflow series, and then the monthly variable threshold level was used to identify drought events for both the natural (simulated) and human-influenced (observed) series in the disturbed period.

3.2.2. Concept of drought termination

Fig. 6 shows a conceptual definition and statistical characteristics of the drought termination phase (Parry et al., 2016; Margariti et al., 2019). In this study, hydrological drought termination was mainly characterised by its starting and ending time, duration, deficit volume, and rate of recovery. The drought maximum intensity (MI) corresponds to the maximum monthly drought deficit volume during a drought event, which divides a drought event into two parts, development and termination phases, and is calculated with:

$$MI(i)=Max\left[Threshold(t)-Q(t)\right],\ if\ Q(t)<Threshold(t) \tag{6}$$

Where, *MI(i)* is the maximum intensity of a drought event *i*, *Q(t)* is the streamflow value for month *t* in drought *i*, *Threshold(t)* is Q_{70} for the same month *t* in drought *i*. The start month of the drought termination phase (DT_{start}) for each drought event is the month when the MI is reached, and the end month of the drought termination phase (DT_{end}) is the last month of the drought event. Therefore, a drought and its termination phase end at the same point in time. The drought termination duration (DT_{dur}) is the number of months between DT_{start} and DT_{end} and is defined by:

$$DT_{dur}(i)=DT_{end}(i)\text{-}DT(i)_{start}+1 \tag{7}$$

Where, $DT_{dur}(i)$ is the drought termination duration for drought *i*, $DT_{start}(i)$ and $DT_{end}(i)$ are start and end months of drought termination phase for drought *i*. The drought termination deficit volume (DT_{def}) is the accumulated deficit volume between DT_{start} and DT_{end} for a given drought event and is calculated with:

$$DT_{def}(i)=\sum_{t=DT_{start}(i)}^{DT_{end}(i)} D_{def}(t) \tag{8}$$

Where, $DT_{def}(i)$ is the total drought termination deficit volume for drought i, $D_{def}(t)$ is the drought deficit volume for month t in drought i. The drought termination rate (DT_{rate}) refers to the maximum intensity divided by the drought termination duration for each event and reflects the rate at which the basin system recharges and returns to non-drought levels. This calculation is illustrated in equation (9)

$$DT_{rate}(i) = \frac{MI(i)}{DT_{dur}(i)} \tag{9}$$

Where, $DT_{rate}(i)$ is the drought termination rate for drought i, $MI(i)$ and $DT_{dur}(i)$ are the maximum intensity and termination duration for drought i.

3.2.3. Run theory

The run theory is a common approach used for identifying propagation characteristics from the drought time series (Yevjevich, 1967). The identification process mainly consists of three steps. The first step is to set three threshold levels, including X_0, X_1, and X_2 ($X_1 > X_0 > X_2$). In this study, X_0, X_1, and X_2 were derived from the 70th, 50th, and 90th percentiles of the monthly duration curves. When streamflow of one month is lower than X_0, this month is initially judged to be drought. The second step is removing minor droughts. If only one month's streamflow is between X_0 and X_2, and no drought occurred before or after this month, it is not considered as a drought event and will be removed. The final step is to combine droughts. When two adjacent drought events are separated by only one month, and streamflow of that month is lower than X_1, then, these two droughts are merged into one drought event. Drought duration is the sum of the two drought durations plus one month. Drought deficit is the sum of the two drought deficits. Otherwise, they are two independent drought events. It is worth noting that minor droughts (duration < 2 month) are removed in this study, because it is difficult to extract the drought development and drought termination phase for minor droughts (Wu et al., 2019).

3.3. Quantifying the impact of human activities on hydrological drought termination

Characteristics of drought termination (e.g., DT_{dur}, DT_{def}, and DT_{dur}) can be extracted based on the TLM_v method and the conceptual definition of drought termination. To estimate the percentage changes in hydrological drought termination metrics due to human influence, the above-mentioned drought termination metrics of the human-influenced data (X_{obs}) and those of the natural data (X_{sim}) were compared using the follow equation:

$$I_h = \frac{X_{obs} - X_{sim}}{X_{sim}} \times 100\% \tag{10}$$

Where I_h is the percentage change in a certain hydrological drought termination characteristic due to human activities, X_{obs}, and X_{sim} is the average value of a certain hydrological drought termination characteristic over all events. A value of $I_h > 0$ means that human activities aggravate hydrological drought termination; a value of $I_h < 0$ means that human activities alleviate hydrological drought termination (Jiang et al., 2019).

Besides, in order to further explore the human influence on different duration drought events, we divided drought events into two scenarios. Scenario 1: the shorter hydrological drought events, whose durations are shorter than value *D*. Scenario 2: the longer hydrological drought events, whose durations are longer than value *D*. Here, *D* was calculated by averaging the total duration of the hydrological drought events from the natural (simulated) drought series of all the human-influenced catchments during disturbed period. The division was necessary, because human activities may have different influence on different kinds of drought events.

4. Results

4.1. Natural streamflow reconstruction

The comparison of the results for the natural streamflow series (simulated by VIC model) and the observed streamflow series showed that the accuracy of the reconstructed streamflow satisfied the requirements of this study (Table 4 and Fig. 7). Because of the different occurrence times of change points in different catchments, the corresponding calibration and validation periods were also different. The values of *NSE*, *LogNSE*, *BIAS*, and *CC* for the Xiaochengzi catchment were 0.73, 0.75, 1.14%, and 0.90 during the calibration period (1964–1988) and 0.87, 0.74, 2.36%, and 0.95 during the validation period (1989–1998). The *NSE* values for the Dianzi catchment during the calibration period (1964–1974) and the validation period (1975–1979) were 0.81 and 0.73, respectively; the *LogNSE* values were 0.77 and 0.75, respectively; the *BIAS* values were 1.81% and 7.27%; and *CC* values were 0.94 and 0.92

respectively. For the Taipingzhuang catchment, the values of *NSE*, *LogNSE*, *BIAS*, and *CC* were 0.90, 0.72, 5.00%, 0.95 and 0.82, 0.80, 5.47%, 0.91 for the calibration period (1964–1974) and validation period (1975–1979) respectively.

4.2. Identification of hydrological drought termination characteristics

The Dianzi and Taipingzhuang catchments (Fig. 8) were selected as examples to illustrate the process of identification of hydrological drought termination characteristics. The variable threshold method was first used to identify hydrological drought events, and then drought termination characteristics were extracted using the concept of drought termination. Drought and drought termination metrics, including the drought duration (D_{dur}), drought deficit volume (D_{def}), drought maximum intensity (MI), drought termination duration (DT_{dur}), drought termination deficit volume (DT_{def}), and drought termination rate (DT_{rate}) during disturbed period were summarised in Table 6 (natural series), Table 7 (human-influenced series), and Fig. 9. Differences of these metrics between observed and simulated series during undisturbed period were summarised in Table 5. In addition, the seasonality of the drought termination starts and ends of the two series in the four catchments was illustrated in Fig. 10. For the natural series (Table 6), the mean DT_{dur} values for the four catchments were 2.68, 2.12, 1.90, and 2.41 months, respectively. The mean DT_{def} and DT_{rate} values for the four catchments were 10.11, 2.78, 7.52, 2.24 mm, and 2.78, 1.56, 3.34, 0.88 mm/month, respectively.

For the three human-influenced series (Table 7), namely, the Xiaochengzi, Dianzi, and Taipingzhuang catchments (remember that the Xiqaun catchment was natural catchment), all of these metrics were greatly increased on average in comparison with the natural series. For example, the mean DT_{def} of the Xiaochengzi catchment in the natural series was 2.78, whilst this value reached 26.78 in the human-influenced series, increasing by more than 10 times. Therefore, it is necessary to compare the hydrological drought termination metrics of natural and human-influenced series to quantify the impact of human activities on the hydrological drought termination phase.

In addition, drought and drought termination characteristics of scenarios 1 and 2 in natural (simulated) and observed series were identified and compared to consider difference of the impacts of human influence on shorter duration and longer duration droughts. For the sake of brevity, Dianzi and Taipingzhuang catchments were selected as examples (Table 8 and Fig. 11) to show the results. For scenario 1 with the shorter droughts, number of shorter droughts in Dianzi catchment decreased from 15 in natural series to 3 in human-influenced series, similar changes also appeared in Taipingzhuang catchment, which means human activities led longer droughts. Drought and drought termination characteristics of human-influenced series were less than (Dianzi) or equal (Taipingzhuang) to those of natural series. For scenario 2 with longer droughts, number of longer droughts in Dianzi catchment increased significantly. Taipingzhuang catchment had the same number of longer droughts in natural and human-influenced series. While, all drought and drought termination characteristics increased in human-influenced series, which means human activities aggravated the drought and drought termination severity. These results revealed that human activities mainly impact duration of shorter droughts and led more of them became longer droughts. As for the longer droughts, all their severity (DT_{dur}, DT_{def}, and DT_{rate}) increased due to human influence. It is necessary, therefore, to classify drought events to analysis, because the impact of human activities on the shorter duration drought and longer duration drought may be quite different.

4.3. Quantification of the impact of human activities on hydrological drought termination

Table 9 and Fig. 9 show that human activities had considerable influences on drought termination for the three catchments, namely, Xiaochengzi, Dianzi, Taipingzhuang catchments. Fig. 10 revealed that the seasonality of drought termination starting (DT_{start}) and ending (DT_{end}) was also shifted due to human activities.

Fig. 9 shows that the median, upper quartile, and upper value of DT_{dur} in the three human-influenced catchments increased significantly. The overall increases in the DT_{dur} of the three catchments were 230%, 73%, and 192%, respectively (Table 9). An increase in the DT_{dur} means that it will take a longer time for a catchment to recharge and return to non-drought level. Fig. 9 also shows that all quartiles values of

DT_{def} in the three human-influenced catchments increased significantly. The overall increases in DT_{def} for the three catchments were 865%, 170%, and 404%, respectively (Table 9). An increase in DT_{def} means that a catchment system needs more water supply to end a drought event. Human activities aggravated drought termination, as also manifested in increasing drought termination rates. The Dianzi catchment had the largest increase of 35%, followed by the Xiaochengzi and Taipingzhuang catchments, which had increases of 26% and 21%, respectively (Table 9).

The impact of human activities was also seen in shifts in the seasonality of drought termination starting and ending. Fig. 10 shows that DT_{start} tended to occur more often in the summer for human-influenced series than that for natural series and the occurring probabilities of DT_{start} were 86%, 100%, and 76% for the three catchments. However, the above probabilities were only 25%, 67%, and 36% for the natural series. In addition, the occurring probabilities of DT_{end} in the three catchments in autumn increased from 25%, 47%, and 14%, respectively, for the natural data to 57%, 63%, and 36%, respectively, for the human-influenced data. Fig. 11 shows human activities caused time of DT_{start} of both two scenarios for the three catchments (at the left of each figure in Fig.11) shifted to summer, with probabilities of 100%, 100%, and 50% in scenario 1 (shorter duration droughts) and 85.7%, 100%, and 100% in scenario 2 (longer duration droughts). While, human influence on changes of timing of DT_{end} (at the right of each figure in Fig.11) of the two scenarios varied in different catchments. DT_{end} of scenario 2 of all the three catchments focused on autumn, with probabilities of 60%, 71%, and 73%. DT_{end} of scenario 1 for Xiaochengzi catchment shifted from summer (50%) to autumn (100%) and that for Dianzi catchment focused on summer (100%). Different with the two catchments, DT_{end} of scenario 1 for Taipingzhuang catchment mainly shifted to summer and winter, with frequency of 50% and 40%.

4.4. Relationship between changes in hydrological drought and those in drought termination

Fig.12 shows that changes of drought termination characteristics (DT_{dur}, DT_{def}, and DT_{rate}) have positive correlations with those in hydrological drought metrics (D_{dur}, D_{def}, and MI) on average. DT_{dur} (or DT_{def}) is a sub-process of D_{dur} (or D_{def}), so there will be a close relationship between changes in these two metrics (i.e., D_{dur} and D_{def}). DT_{rate}, which is calculated by MI and DT_{dur} (Fig. 6), also kept consistent with the change of MI. Among all three altered catchments, the drought and drought termination characteristics of the Xiaochengzi catchment had the largest changes.

Further comparisons (Fig. 12(a), (e) and (i)) revealed that, ratio of changes in drought metrics (e.g. D_{dur}) and those in drought termination metrics (e.g. DT_{dur}) varied in different catchments. Climate and catchment characteristics may be a reason, and difference of predominant human activity (land use change, reservoir regulations, or human water withdrawal) within each catchment may also cause the above differences. Given that the number of catchments considered in this study was limited, more case studies are needed to further explore the relationship between changes in drought termination metrics and those in drought metrics.

5. Discussion

5.1. Human influence on hydrological drought termination

In this study, a comprehensive approach was proposed for identification and quantification of hydrological drought termination characteristics of natural and human-influenced series. Comparison of these two series showed that human activities such as human water withdrawal, reservoir regulations, and land use change, influenced the hydrological drought termination phase directly or indirectly.

Human water withdrawal for agricultural irrigation, urban water supply, or industrial production significantly reduced the available water in rivers, and then led to longer drought termination durations and larger drought termination deficits (Fig. 8 and 9, and Table 9). Fig. 4 shows that socioeconomic data of the study area increased sharply in the disturbed period (1980–2016). The rapid development of agriculture (Figs. 4(c) and (d)) consumed a large amount of water resources for irrigation, drinking water for livestock, and other applications. In 21st century, population of the study area has stopped increasing but remained at a high level (Fig. 4(a)), leading to a sustained increase in domestic water. The GDP of the study region (Fig. 4(b)) experienced rapid growth after the national economic opening policy was implemented in 1979 (In 2016, the GDP was more than 200 times greater than that of

1979). The secondary and tertiary industries (agriculture belongs to the primary industry) that supported the rapid growth of GDP also caused a massive consumption of water resources. All of these human water withdrawals aggravated hydrological drought termination severity.

Reservoir regulations, as another factor affecting hydrological drought, has influence on hydrological drought termination time. Dahushi reservoir (storage capacity: 1.2×10^8 m^3), located in Dianzi catchment, began to store water in 1980 and focus on agricultural irrigation. Fig. 10(c) shows that probability of DT_{start} occurring during the summer period (from June to August) and DT_{end} occurring during the autumn period (September to November) increased significantly after the construction of Dahushi reservoir. The reason is that reservoir regulations usually maintained storage in spring and winter, and then released water in summer and autumn to guarantee agriculture irrigation (Yong et al., 2013; Ren et al., 2014). These regulations and the concentrated precipitation in June-September (summer and autumn) caused hydrological drought termination starting on summer and ending on autumn more frequently.

Shifts of the seasonality of drought termination starting and ending in the other two catchments, Xiaochengzi and Taipingzhuang catchments, were more related to changes of land use. Fig. 3 shows that areas of cropland and urban kept increasing, and those of forest land, grassland, water, and unused land decreased significantly after 1980. Increase of cropland means strengthening of agricultural activities. Yong et al. (2013) pointed out that the study region (Fig. 1) belonged to semi-arid areas in northern China, which caused the water demand of agriculture production mainly relies on human irrigation instead of natural precipitation. The periodicity of agricultural activities (farmers generally plant seeds in May and harvest crops in October) led to the shifts of seasonality of hydrological drought termination. In high-flow years (drought events of these two catchments in 1990s, as can be seen in Figs. 8(b) and (d), streamflow could meet the water demand of crops, and hydrological drought event occurred less frequently. Whereas, in moderate- or low-flow years (drought events of these two catchments in 2000–2016, as can be seen in Figs. 8(b) and (d)), hydrological drought events occurred frequently and even lasted for several years.

In addition, we also analysed differences of human influence on drought termination time of the two scenarios (Fig. 11). Time of DT_{start} of both two scenarios (left column graphs in Fig.11) shifted to summer, while, changes of timing of DT_{end} (right column graphs in Fig.11) of the two scenarios varied in different catchments. The reason why the DT_{start} shifts to summer is that, agriculture activities (May to October) and reservoir regulations were mainly concentrated on summer and may cause appearance of max drought intensity (MI), which also means the start of drought termination phase. While, different dominant human activities in different catchments led to different changes in DT_{end} time. In Xiaochengzi catchment (Fig. 11(b)), agriculture irrigation (the dominant human activities) caused DT_{end} of scenario

1 shifting from other seasons to autumn, and that of scenario 2 focusing on summer and autumn. In Dianzi catchment (Fig. 11(c)), reservoir regulations (the dominant human activities) often finished in autumn, the release water helped for DT_{end} of scenario 2 shifting to this season. Whereas, DT_{end} of scenario 1 of Dianzi catchment only appeared in summer, because adequate precipitation in this season may quickly relieve hydrological drought events.

5.2. Uncertainties and limitations

Though the approach proposed in this study was used for identification and quantification of hydrological drought termination characteristics of natural and human-influenced series, this approach still has some uncertainties and limitations.

Different drought assessment methods or different types of drought have their own drought termination criteria, which led to a lack of a unified definition of drought termination (Heim Jr. and Brewer, 2012; Parry et al., 2016). Thus, different definitions may have different identification of the drought termination characteristics. It is worth to noting that the drought termination concept (proposed by Parry et al., 2016) followed by this study has already some applications. Wu et al. (2019) and Margariti et al. (2019) have used this concept to explore human influence on hydrological termination phase. Based on their studies, we also chose this concept for identification of drought termination characteristics. However, we should also pay attention to the uncertainty of this definition. River flows are integrative in space and time, so drought termination as defined in this method could occur without fully compensating for the deficit accumulated during drought development (Parry et al., 2016), which will lead to uncertainty on identified drought termination characteristics (e.g. drought termination time). In addition, the drought termination process is a complex process driven by multiple mechanisms. The impact of the synergy or nonlinear caused by more than one human activity in a certain basin will also have uncertain influence on this definition of drought termination. Thus, a larger sample size of observed drought terminations and more applications are needed to improve the stability of this definition of drought termination.

The approach proposed in this study is based on VIC hydrological model and various hydrological model types can be chosen in this approach, such as a distributed or lumped model, a physically based model, a conceptual model, or even a stochastic model (Van Loon and Van Lanen, 2013). While, any study using a hydrological model will have associated uncertainties (Beven, 1993; Gupta et al., 1998; Walker et al., 2003). In this study, the Xiquan catchment was a natural catchment and was selected to verify the accuracy of the results for the VIC model simulation and drought characteristics identification. Table 4 and Fig. 7(a) show that NSE, LogNSE, BIAS and CC values were 0.78, 0.77, 9.19%, and 0.91 in the calibration period (1965-1974), 0.79, 0.85, –5.8%, and 0.92 in validation period (1975-1979), and 0.77, 0.86, –0.14 and 0.88 in simulation period (1980–2016) respectively. These results prove that the accuracy of the reconstructed streamflow during the disturbed period can satisfy the requirements of this study.

Drought process is closely related to the low-flow process, and the simulation uncertainty of the low-flow process affects the identification results of the drought termination. Figs. 8(a) and (c), and Table 5 indicate that average deviations of drought metrics between observed and simulated series in undisturbed period were 1.55%, 2.51%, and 3.39% for drought duration, deficit, and maximum intensity, and 0.41%, 1.92%, and 2.62% for drought termination duration, deficit, and rate. Though the average deviations were far from those in disturbed period (e.g., 601%, 1376%, 209%, 230%, 865%, and 35% in Xiaochengzi catchment), more works are needed to reduce uncertainty of simulation on identification results of the drought termination.

Meanwhile, re-wetting and recovery are not always simulated well in hydrological models and therefore the processes most relevant to drought termination time may have larger uncertainties (Birkel et al., 2011). Comparison of drought termination time between simulated and observed series in Xiquan catchment (a natural catchment) revealed simulation uncertainties led to some deviations on the identification of drought termination time. Fig. 10(a) shows that frequency of DT_{start} in spring for simulated series was 3% lower than that for observed series. Fig. 11(a) also shows that, for drought of scenario 1, frequencies of both DT_{start} and DT_{end} in spring for simulated series were 4% and 5% lower than those for observed series. For drought of scenario 2 (Fig. 11(a)), underestimation and overestimation of frequencies of DT_{end} appeared in winter and spring seasons for simulated series, respectively.

Therefore, we must realize that simulation uncertainty will impact identification of the termination time of some drought events, and further work needs to improve the accurate capture of the drought termination time in the simulation series.

Finally, it is important to consider impact of non-stationarity in the future research. Non-stationarity of streamflow may affect the selection of the threshold level or the calculation of the standardized indices, and then lead to uncertainty on identification results of drought termination characteristics. Fortunately, in recent studies, some frameworks or methods that consider non-stationarity could more accurately and effectively reveal the impact of human activities on hydrological drought and drought termination (Wanders and Wada, 2015; Zou et al., 2018). Future studies, therefore, should focus on building a more comprehensive framework that considers non-stationarity to evaluate the impact of human activities on the hydrological drought termination, which will help us gain a deeper understanding of how hydrological process changes in changing environment.

6. Conclusions

In this study, a comprehensive approach combining an 'observed–simulated' comparison approach, the concept of drought termination, and the variable threshold level method was proposed and applied for identification and quantification of the hydrological drought termination characteristics of natural series and human-influenced series in Laohahe basin. The results showed that human water withdrawal for agricultural irrigation, urban water supply, or industrial production led to longer drought termination durations and larger drought termination deficits and rates, with maximum increases of 230%, 865%, and 35%, respectively. Land use change and reservoirs regulations caused changes of seasonality of drought termination starting and ending. The preferred season for DT_{start} and DT_{end} was shifted to summer and autumn, respectively.

The findings of this study help understanding how human activities alter hydrological drought termination severity (drought termination duration, deficit, and rate), and time (drought termination start or end). Although the Laohahe basin was selected as a case study in this paper, the proposed approach can be applied in other regions as well. Systematic knowledge of the impacts of human activities on hydrological drought termination is crucial for improving the forecasting of drought recovery and establishing a reliable drought early warning system. Meanwhile, future studies should focus on constructing a comprehensive framework that considers non-stationarity, and then separating impacts of different kinds of human activities (land use change, reservoir regulations, and human water withdrawal) on the hydrological drought termination process, which will provide valuable information for adaptive responses to hydrological drought.

Acknowledgments

This work was financially supported by the National Key Research and

Development Program approved by Ministry of Science and Technology, China (2016YFA0601504); the National Natural Science Foundation of China (51979069); the Fundamental Research Funds for the Central Universities (B200204029); the Programme of Introducing Talents of Discipline to Universities by the Ministry of Education and the State Administration of Foreign Experts Affairs, China (B08048); the National Natural Science Foundation of Jiangsu Province, China (BK20180512).

References

Adam, J.C., Haddeland, I., Su, F., Lettenmaier, D.P., 2007. Simulation of reservoir influences on annual and seasonal streamflow changes for the Lena, Uenisei, and Ob' rivers. J. Geophys. Res. Atmos. 112(D24), D24114.

Ahmadi, B., Ahmadalipour, A., Moradkhani, H., 2019. Hydrological drought persistence and recovery over the CONUS: A multi-stage framework considering water quantity and quality. Water Res. 150, 97–110.

Andreadis, K.M., Lettenmaier, D.P., 2006. Trends in 20th century drought over the continental United States. Geophys. Res. Lett. 33, L10403.

Antofie, T., Naumann, G., Spinoni, J., Vogt, J., 2014. Estimating the water needed to end or ameliorate the drought in the Carpathian region. Hydrol. Earth Syst. Sc. 11, 1493–1527.

Bell, V. A., Davies, H. N., Kay, A. L., Marsh, T., Brookshaw, A., Jenkins, A., 2013. Developing a large-scale water-balance approach to seasonal forecasting: application to the 2012 drought in Britain. Hydrol Process. 27(20), 3003-3012.

Beven, K., 1993. Prophecy, reality and uncertainty in distributed hydrological modelling. Adv. Water Resour. 16(1), 41–51.

Birkel, C., Soulsby, C., Tetzlaff, D., 2011. Modelling catchment-scale water storage dynamics: reconciling dynamic storage with tracer-inferred passive storage. Hydrol Process. 25(25), 3924-3936.

Byun, H., Wilhite, D. A., 1999. Objective quantification of drought severity and duration. J. Clim. 12(9), 2747-2756.

Chen, X., Li, F-W, Wang, Y-X, Feng, P., Yang, R.Z., 2019. Evolution properties between meteorological, agricultural and hydrological droughts and their related driving factors in the Luanhe River Basin, China. Hydrol. Res. 50 (4), 1096–1119.

Dai A., 2011. Drought under global warming: A review. Wiley Interdiscip. Rev. Clim. Change 2(1), 45–65.

Dehghani, M., Zargar, M., 2019. Probabilistic hydrological drought index forecasting based on meteorological drought index using Archimedean copulas. Hydrol. Res. 50 (5), 1230–1250.

Fleig, A. K., Tallaksen, L. M., Hisdal, H., Demuth, S., 2006. A global evaluation of streamflow drought characteristics. Hydrol. Earth Syst. Sci. 10, 535–552.

Forzieri, G., Feyen, L., Rojas, R., Flörke, M., Wimmer, F., Bianchi, A., 2014. Ensemble projections of future streamflow droughts in Europe. Hydrol. Earth Syst. Sci. 18, 85–108.

Gupta, H.V., Sorooshian, S., Yapo, P.O., 1998. Toward improved calibration of hydrological models: Multiple and noncommensurable measures of information. Water Resour. Res. 34(4), 751–763.

Hannaford, J., Lloydhughes, B., Keef, C., Parry, S., Prudhomme, C., 2011. Examining the large-scale spatial coherence of European drought using regional indicators of precipitation and streamflow deficit. Hydrol Process, 25(7), 1146-1162.

Heim, R.R. Jr., Brewer, M.J., 2012. The global drought monitor portal: The foundation for a global drought information system. Earth Interact. 16(15), 1–28.

Hisdal, H., Stahl, K., Tallaksen, L. M., and Demuth, S., 2001. Have streamflow droughts in Europe become more severe or frequent? Int. J. Climatol. 21(3), 317–333.

Jiang, S., Ren, L., Yong, B., Singh, V. P., Yang, X., Yuan, F., 2011. Quantifying the effects of climate variability and human activities on runoff from the Laohahe Basin in northern China using three different methods. Hydrol. Process. 25, 2492–2505.

Jiang, S., Ren, L., Yong, B., Fu, C., Yang, X., 2012. Analyzing the effects of climate variability and human activities on runoff from the Laohahe Basin in northern China. Hydrology. Res. 43(1–2), 3–3.

Jiang, S., Ren, L., Xu, C., Yong, B., Yuan, F., Liu, Y., Zeng, X., 2018. Statistical and hydrological evaluation of the latest integrated multi-satellite retrievals for GPM (IMERG) over a midlatitude humid basin in South China. Atmos. Res. 214, 418–429.

Jiang S., Wang M., Ren L., Xu, C., Yuan, F., Liu, Y., Shen, H., 2019. A framework for quantifying the impacts of climate change and human activities on hydrological drought in a semiarid basin of Northern China. Hydrol. Process. 33, 1075–1088.

Jiang S., Wei L., Ren L., Xu, C., Feng Z., Wang M., Zhang L., Yuan F., Liu Y., 2020. Utility of integrated IMERG precipitation and GLEAM potential evapotranspiration products for drought monitoring over mainland China. Atmos. Res. https://doi.org/10.1016/j.atmosres.2020.105141

Kendall, M.G., 1975. Rank Correlation Methods. Charles Griffin, London.

Krysanova, V., Buiteveld, H., Haase, D., Hattermann, F.F, van Niekerk, K., Roest, K., Martınez-Santos, P., M. Schlüter, M., 2008. Practices and lessons learned in coping with climatic hazards at the river-basin scale: Floods and droughts. Ecol. Soc. 13(2).

Lettenmaier, D.P., Gan, T.Y., 1990. Hydrologic sensitivities of the Sacramento-San Joaquin River Basin, California, to global warming. Water Resour. Res. 26, 69–86.

Li, J.Z., Zhang, S.Y., Huang, L.M., Zhang, T., Feng, P., 2020a. Drought prediction models driven by meteorological and remote sensing data in Guanzhong Area, China. Hydrology Research. https://doi.org/10.2166/nh.2020.184

Li, Z.L., Shao, Q.X., Tian, Q.Y., Zhang, L., 2020b. Copula-based drought severity-area-frequency curve and its uncertainty, a case study of Heihe River basin, China. Hydrology Research. https://doi.org/10.2166/nh.2020.173

Liang, X., Lettenmaier, D.P., Wood, E.F., Burges, S.J., 1994. A simple hydrologically based model of land surface water and energy fluxes for GSMs. J. Geophys. Res. Atmos. 99(D7),14415–14428.

Liang, X., Guo, J., Leung, L.R., 2004. Assessment of the effects of spatial resolutions on daily water flux simulation. J. Hydrol. 298, 287–310.

Liu, X., Ren, L., Yuan, F., Singh, V.P., Fang, X., Yu, Z., Zhang, W., 2009. Quantifying the effect of land use and land cover changes on green water and blue water in northern part of China. Hydrol. Earth Syst. Sc. 13, 735–747.

Liu, Y., Ren, L., Zhu, Y., Yang, X., Yuan, F., Jiang, S., Ma, M., 2016. Evolution of hydrological drought in human disturbed areas: A case study in the Laohahe basin, Northern China. Adv. Meteorol. 2016, 1–12.

Lin, Q., Wu, Z., Singh, V. P., Sadeghi, S. H. R., He, H., and Lu, G., 2017. Correlation between hydrological drought, climatic factors, reservoir operation, and vegetation cover in the Xijiang Basin, South China. J. Hydrol. 549, 512–524.

Ma, M., Ren, L., Yuan, F., Jiang, S., Liu, Y., Kong, H., Gong, L., 2014. A new standardized Palmer drought index for hydrometeorological use. Hydrolog. Process. 28, 5645–5661.

Mann, H. B., 1945. Nonparametric tests against trend. Econometr. J. Econometr. Soc. 13, 245–259.

Margariti, J., Rangecroft, S., Parry, S., Wendt, D. E., Van Loon, A. F., 2019. Anthropogenic activities alter drought termination. Elementa: Sci. Anthropocene 7(27).

Merz, R., Parajka, J., Bloeschl, G., 2011. Time stability of catchment model parameters: implications for climate impact analyses. Water Resour. Res., 47(2), p.W02531.1-W02531.17.

Mishra, A.K., Singh, V.P., 2010. A review of drought concepts. J. Hydrol. 391(1–2), 202–216.

Palmer, M.A., Liermann, C.A.R., Nilsson, C., Flörke, M., Alcamo, J., Lake, P.S, Bond, N., 2008. Climate change and the world’s river basins: Anticipating management options. Front. Ecol. Environ. 6(2), 81–89.

Pan M., Wood, E.F., Wójcik, R., Mccabe, M.F., 2008. Estimation of regional terrestrial water cycle using multi-sensor remote sensing observations and data assimilation. Remote Sens. Environ. 112(4), 1282–1294.

Pan, M., Yuan, X., & Wood, E. F. (2013). A probabilistic framework for assessing drought recovery. Geophys. Res. Lett. 40(14), 3637-3642.

Parry, S., Prudhomme, C., Wilby, R.L., Wood, P.J., 2016. Drought termination: Concept and characterization. Process. Phys. Geog. 40(6),743–767.

Parry, S., Wilby, R. L., Prudhomme, C., Wood, P. J., Mckenzie, A., 2018. Demonstrating the utility of a drought termination framework: prospects for groundwater level recovery in England and Wales in 2018 or beyond. Environ Res Lett, 13(6).

Pereira, L.S., Cordery, I., Iacovides, I., 2009. Coping with Water Scarcity: Addressing the Challenges. Springer Science & Business Media.

Pettitt, A.N., 1979. A non-parametric approach to the change-point problem. J. R. Stat. Soc. Ser. C. (App. Stat.) 28(2), 126–135.

Rangecroft, S., Van Loon, A.F., Maureira H., Verbist, K., Hannah, D.M., 2019. An observation-based method to quantify the human influence on hydrological drought: upstream–downstream comparison. Hydrolog. Sci. J. 64:3, 276–287.

Ren, L., Yuan, F., Yong, B., Jiang, S., Yang, X., Gong, L., Ma, M., Liu, Y., Shen, H., 2014. Where does blue water go in the semi-arid area of northern China under changing environments? Proc. IAHS, 364, 88–93.

Sarailidis, G., Vasiliades, L., Loukas, A., 2019. Analysis of streamflow droughts using fixed and variable thresholds. Hydrolog. Process. 33, 414–431.

Seneviratne, S. I., Nicholls, N., Easterling, D., Goodess, C.M., Zhang, X., 2012. Changes in climate extremes and their impacts on the natural physical environment, in: Field, C. B., Barros, V., Stocker, T. F., Qin, D., Dokken, D. J., Ebi, K. L., Mastrandrea, M. D., Mach, K. J., Plattner, G.-K., Allen, S. K., Tignor, M., and Midgley, P. M (Eds.), Managing the Risks of Extreme Events and Disasters to Advance Climate Change Adaptation (IPCC SREX Report), Cambridge University Press, Cambridge and New York, pp. 109–230.

Sheffield, J., Wood, E.F., Roderick, M.L., 2012. Little change in global drought over the past 60 years. Nature 491, 435–438.

Tallaksen, L.M., Van Lanen, H.A.(Eds.)., 2004. Hydrological drought: Processes and estimation methods for streamflow and groundwater, Vol. 48. Elsevier.

Van Lanen, H.A.J., Wanders, N., Tallaksen, L.M., Van Loon, A.F., 2013. Hydrological drought across the world: impact of climate and physical catchment structure. Hydrol. Earth Syst. Sci. 17, 1715–1732.

Van Loon, A.F., Van Lanen, H.A.J., 2013. Making the distinction between water scarcity and drought using an observation-modeling framework. Water Resour. Res. 49, 1483–1502.

Van Loon, A.F., 2015. Hydrological drought explained. WIREs Water 2, 359–392.

Van Loon, A. F., Gleeson T., Clark J., et al., 2016. Drought in the Anthropocene. Nature Geosci. 9(2), 89-91.

Van Loon, A.F., Rangecroft S., Coxon G., Breña Naranjo, J.A., Ogtrop, F.V., Van Lanen, H. A., 2019. Using paired basins to quantify the human influence on hydrological droughts. Hydrol. Earth Syst. Sci. 23(3), 1725–1739.

Walker, W.E., Harremoes, P., Rotmans, J., van der Sluijs, J.P., van Asselt, M., Janssen, P., Krayer von Krauss, M.P., 2003. Defining uncertainty: A conceptual basis for uncertainty management in model-based decision support. Integr. Assess. 4(1), 5–17.

Wanders, N., Wada, Y., 2015. Human and climate impacts on the 21st century hydrological drought. J. Hydrol. 208-220.

Watts, G., von Christierson, B., Hannaford, J., Lonsdale, K., 2012. Testing the resilience of water supply systems to long droughts, J. Hydrol. 414, 255–267.

Wu, J., Chen, X., Yu, Z., Yao, H., Li, W., Zhang, D., 2019. Assessing the impact of human regulations on hydrological drought development and recovery based on a ‘simulated-observed’ comparison of the SWAT model. J. Hydrol. 577, 123990.

Xia, J., Yang, P., Zhan, C.S., Qiao, Y.F., 2019. Analysis of changes in drought and terrestrial water storage in the Tarim River Basin based on principal component analysis. Hydrol. Res. 50(2), 761–777.

Yeh, H.F., 2019. Using integrated meteorological and hydrological indices to assess drought characteristics in southern Taiwan. Hydrol. Res. 50 (3), 901–914.

Yevjevich, V. M., 1967. Objective approach to definitions and investigations of continental hydrologic droughts, An. Hydrol. Papers (Colorado State University). No. 23.

Yong, B., Ren, L., Hong, Y., Gourley, J.J., Chen, X., Dong, J.W., Hardy, J., 2013. Spatial-temporal changes of water resources in a typical semiarid basin of North China over the past 50 years and assessment of possible natural and socioeconomic causes. J. Hydrometeor. 14, 1009–1034.

Yuan, F., Wang, B., Shi, C., Cui, W., Zhao, C., Liu, Y., Ren, L., Zhang, L., Zhu, Y., Chen, T., Jiang, S., Yang, X., 2018. Evaluation of hydrological utility of IMERG Final run V05 and TMPA 3B42V7 satellite precipitation products in the Yellow River source region, China. J. Hydrol. 696-711.

Yuan, X., Jiao, Y., Yang, D., Lei, H., 2018. Reconciling the attribution of changes in streamflow extremes from a hydroclimate perspective. Water Resour. Res. 54, 3886–3895.

Zargar, A., Sadiq, R., Naser, B., Khan, F.I., 2011. A review of drought indices. Environ. Rev. 19, 333–349.

Zou, L., Xia, J., She, D., 2018. Analysis of impacts of climate change and human activities on hydrological drought: A case study in the Wei River Basin, China. Water Resour. Manag. 32(4), 1421–1438.

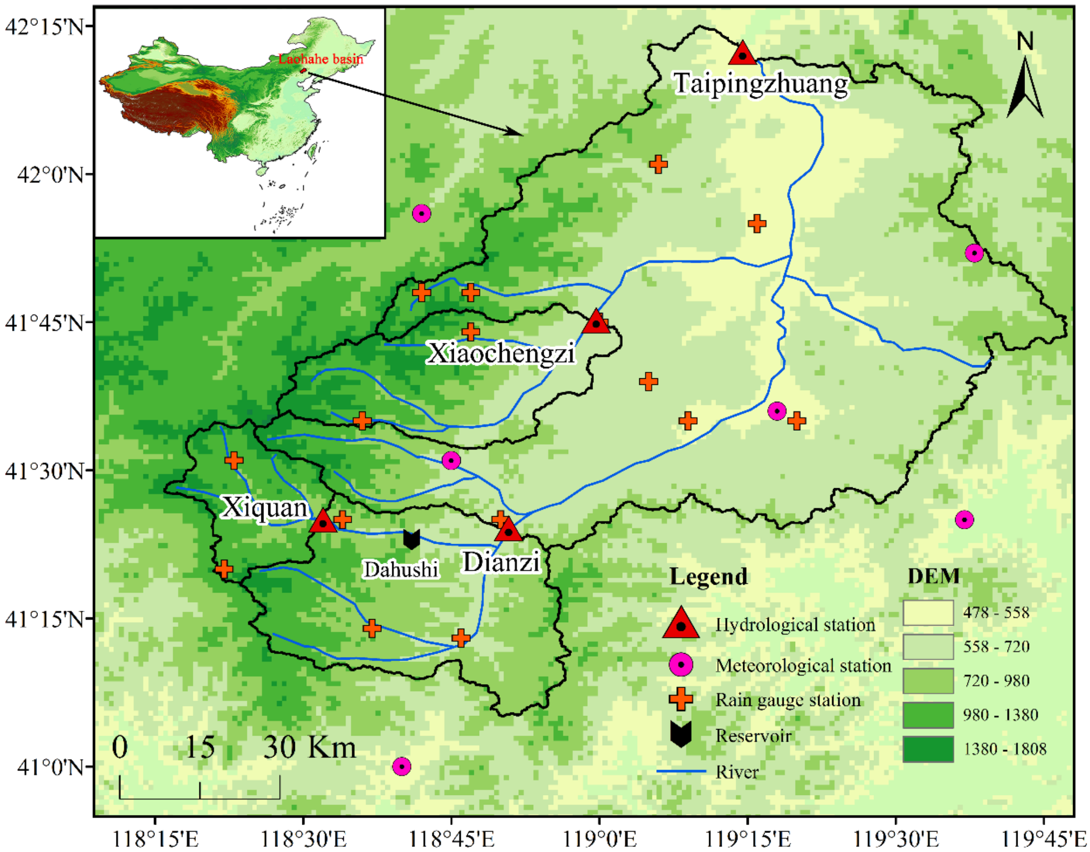

Fig. 1. Location of the study areas and distribution of the hydrological, meteorological, and rain gauge stations.

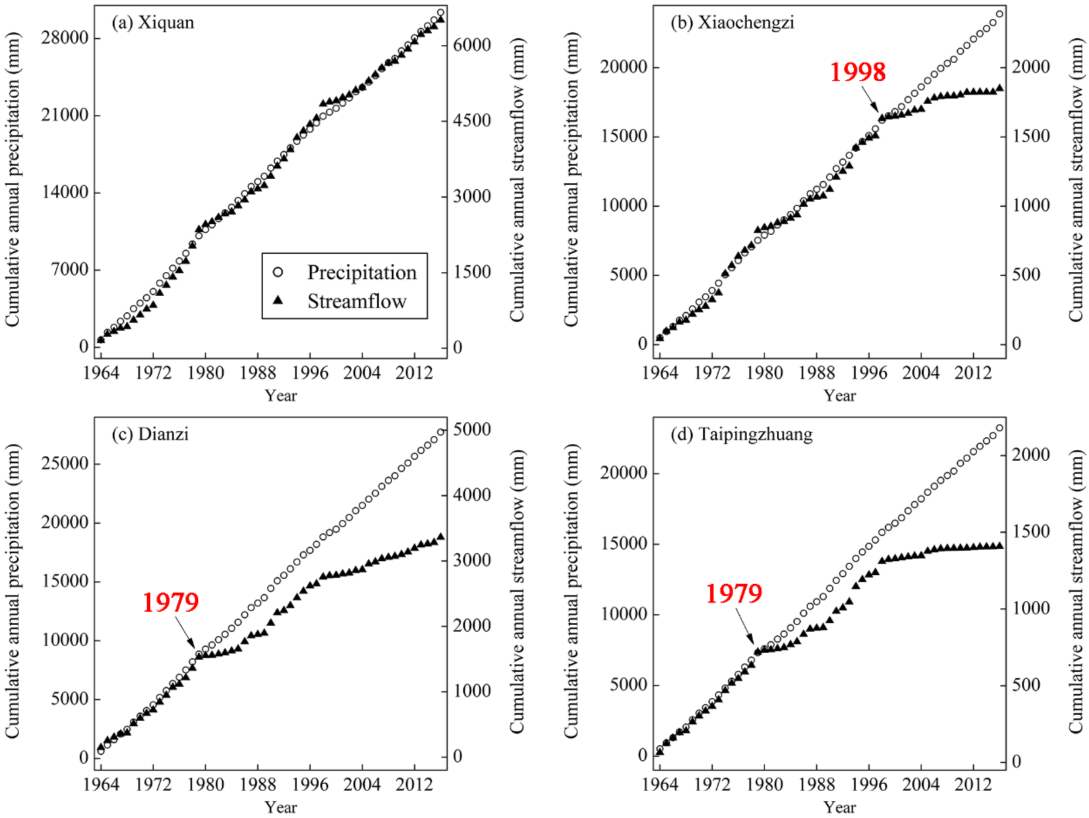

Fig. 2. Double cumulative curves of annual precipitation and streamflow in (a) Xiquan, (b) Xiaochengzi, (c) Dianzi, and (d) Taipingzhuang catchments.

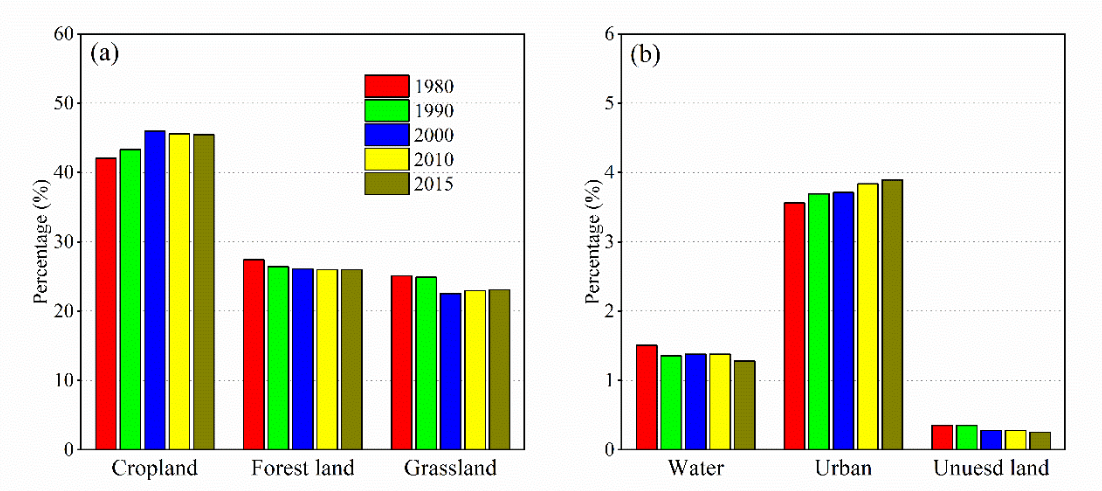

Fig. 3. Land use changes for the study area in the disturbed period: (a) Cropland, Forest land, and Grassland and (b) Water, Urban, and Unused land.

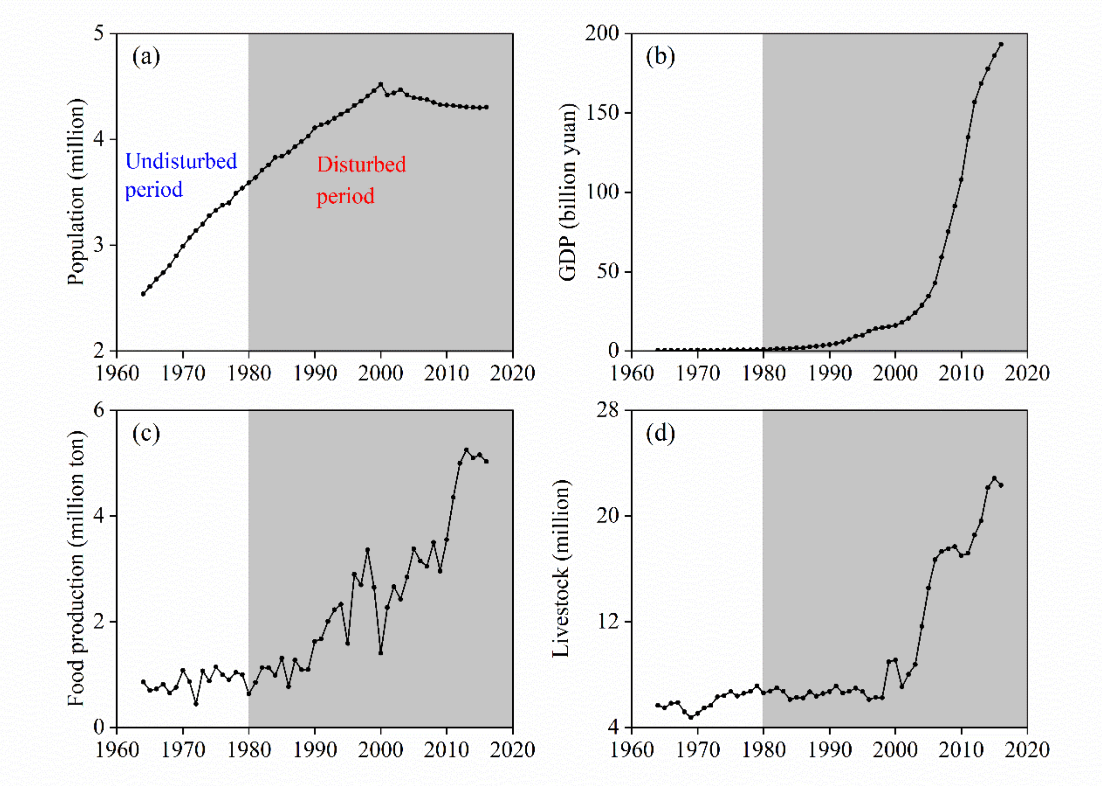

Fig. 4. Changes of socioeconomic data for the study area during 1964–2016 (undisturbed period and disturbed period): (a) population, (b) GDP, (c) food population, and (d) number of livestock.

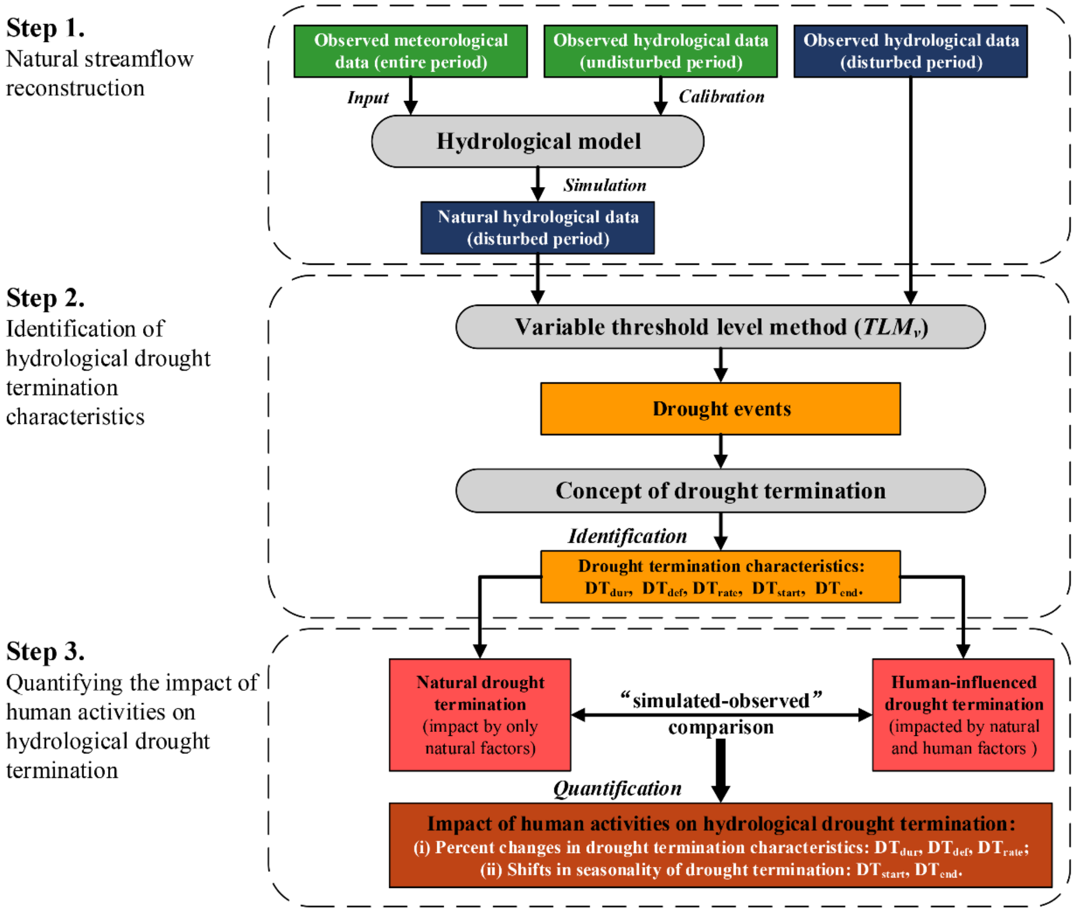

Fig. 5. Proposed approach for identifying hydrological drought termination characteristics and quantifying the impact of human activities on hydrological drought termination.

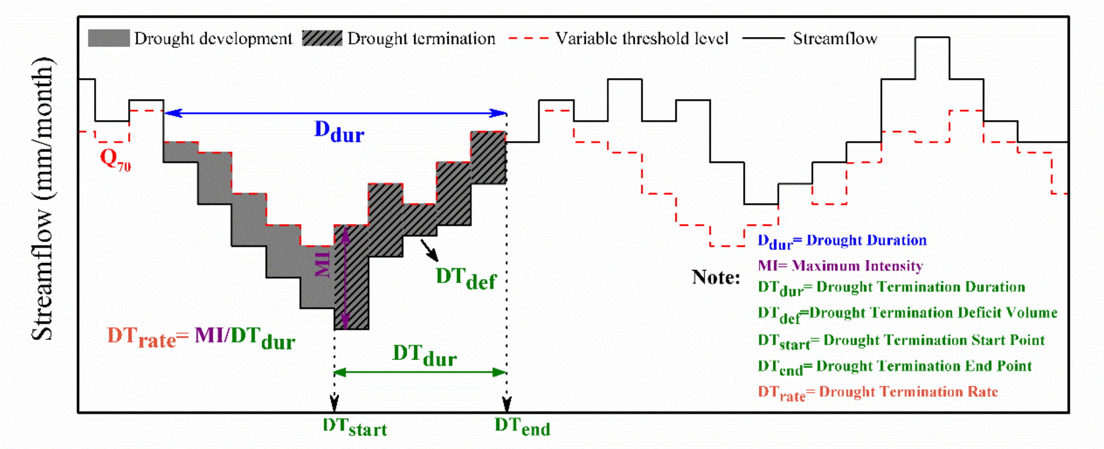

Fig. 6. Definition of drought termination (modified from Parry et al., 2016; Margariti et al., 2019).

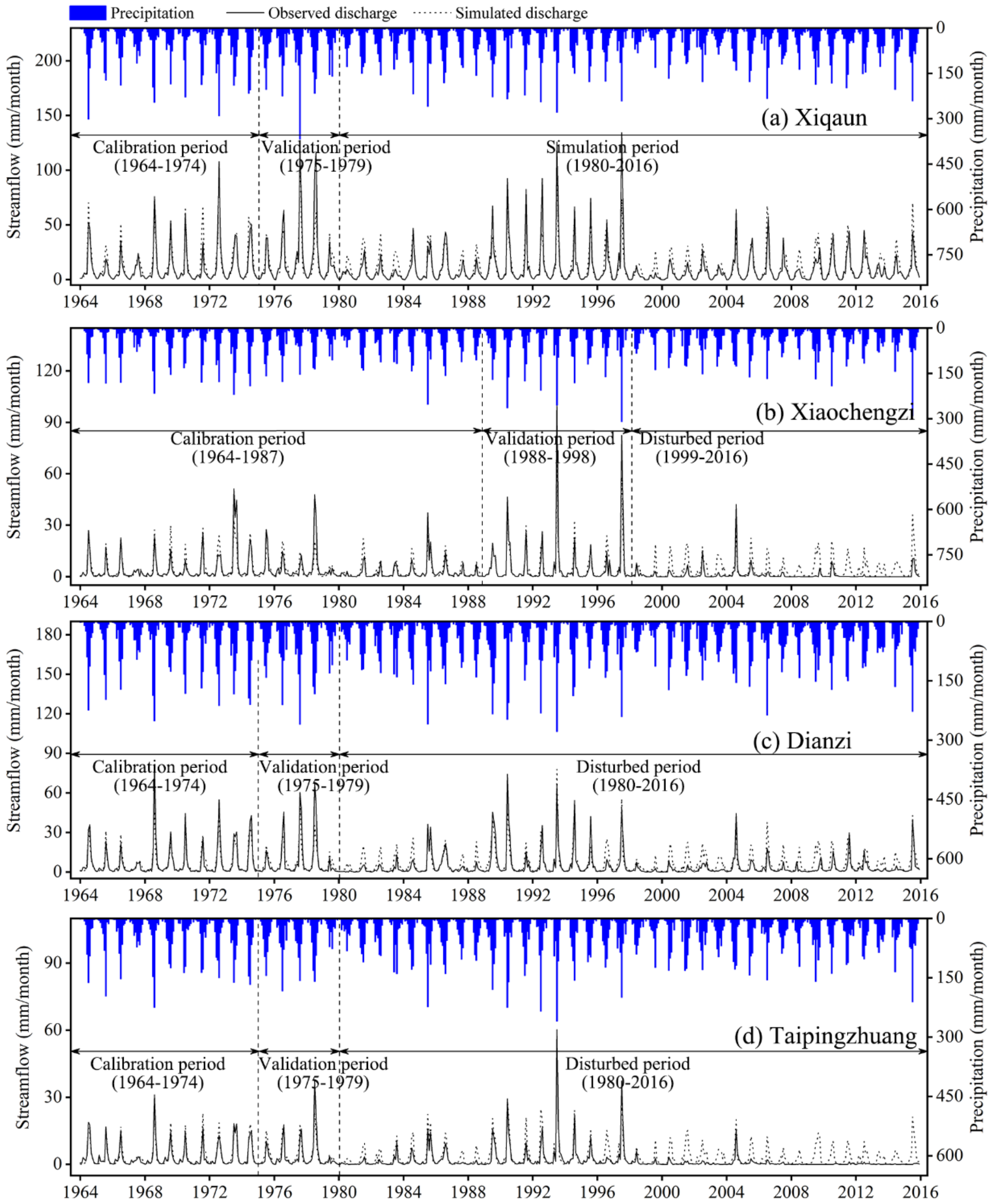

Fig. 7. Comparisons of VIC-simulated and observed monthly streamflow for Xiquan (undisturbed and simulation periods), Xiaochengzi, Dianzi, and Taipingzhuang catchments (undisturbed and disturbed periods).

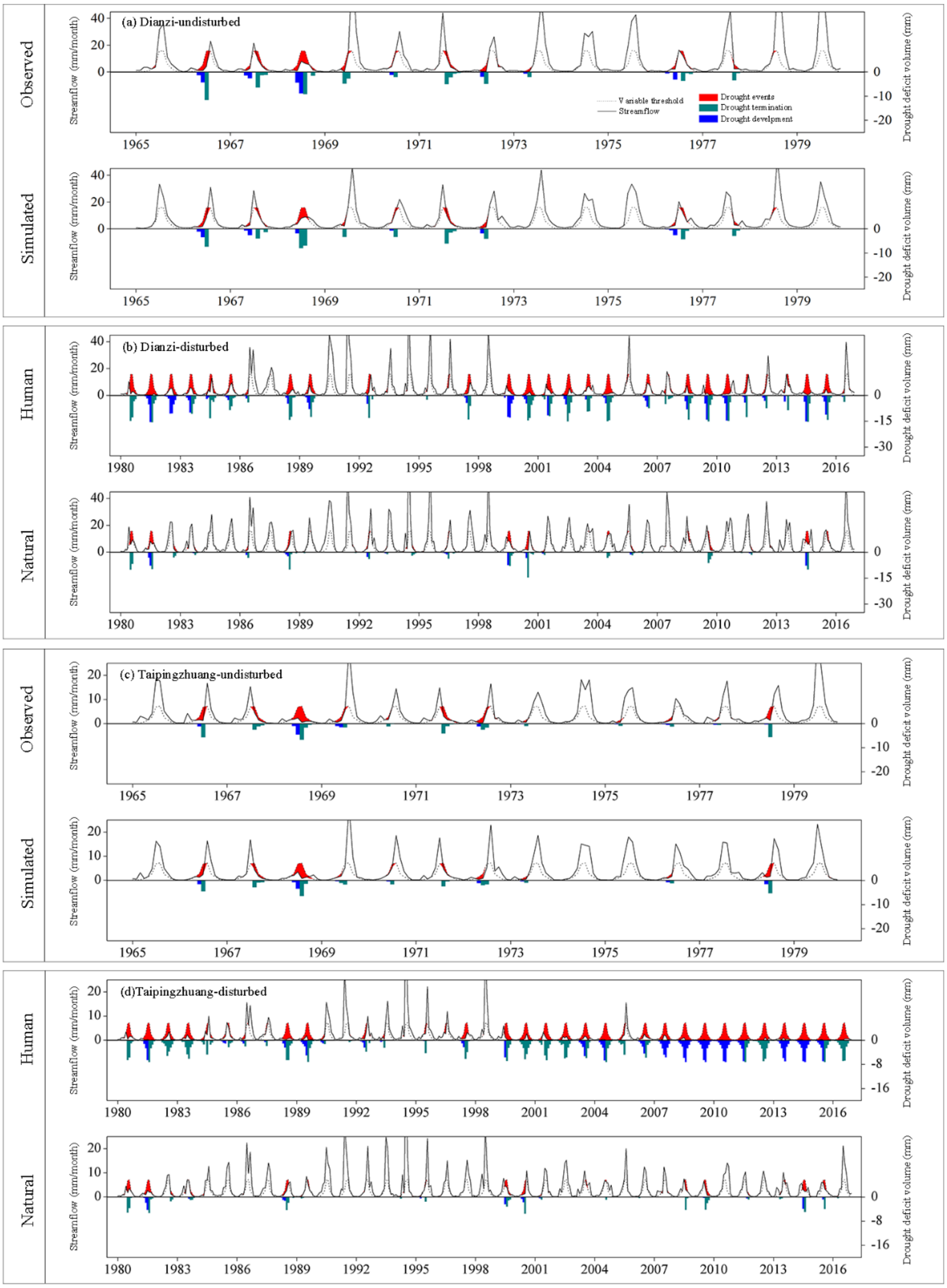

Fig. 8. Identification and comparison of drought termination characteristics for observed and simulated series during undisturbed period, and for human-influenced and natural series during disturbed period in Dianzi and Taipingzhuang catchments.

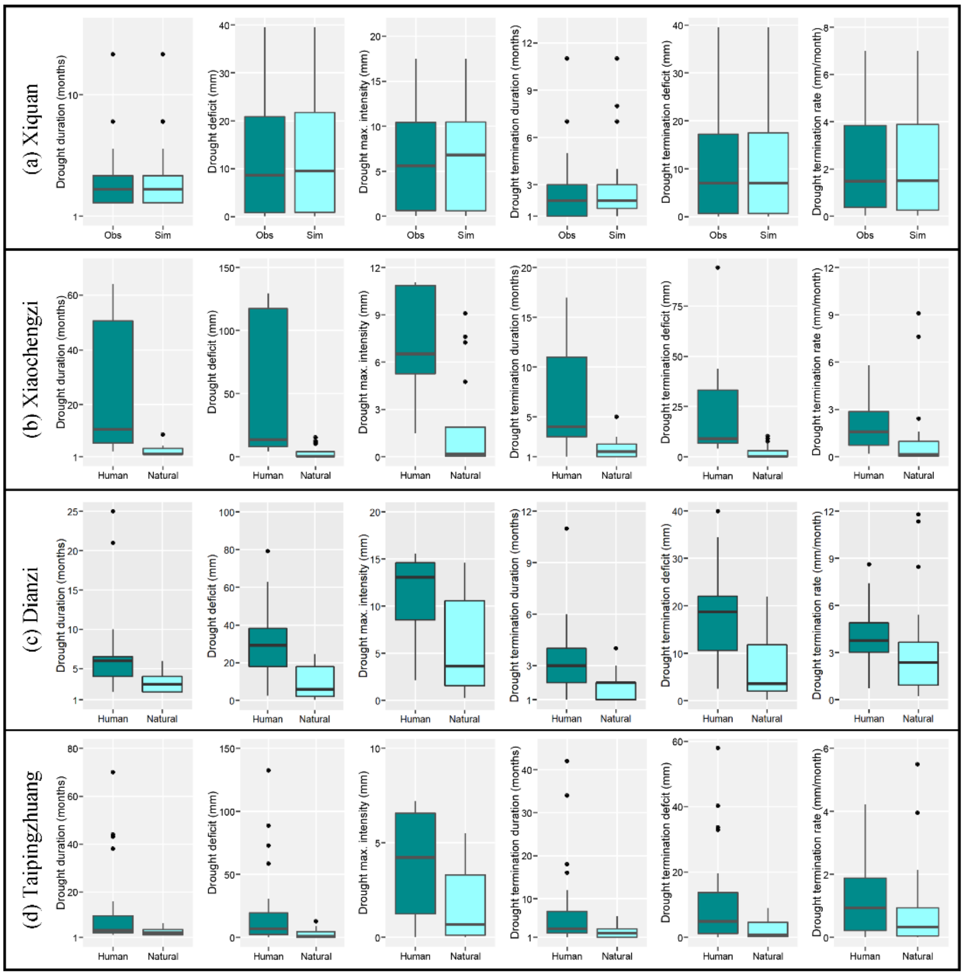

Fig. 9. Boxplots of drought and those of drought termination characteristics for (a) Xiquan (observed (left) and simulated (right) series), (b) Xiaochengzi, (c) Dianzi, and (d) Taipingzhuang catchments (human-influenced (left) and natural (right) series).

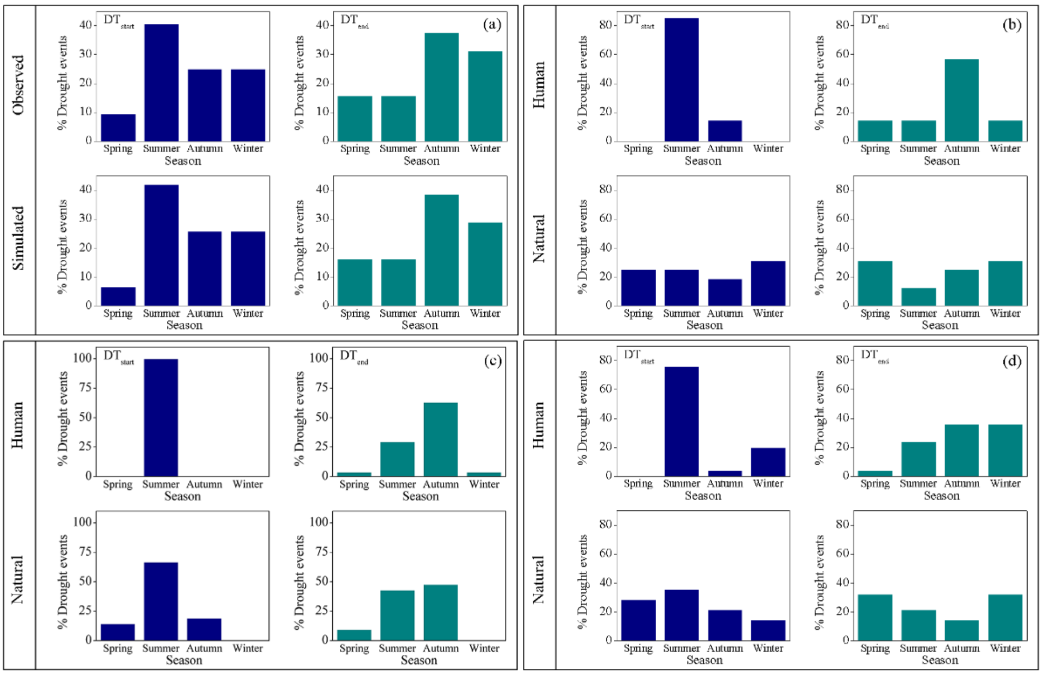

Fig. 10. Changes of seasonality of drought termination starting and ending for (a) Xiquan (observed (top) and simulated (bottom) series), (b) Xiaochengzi, (c) Dianzi, and (d) Taipingzhuang catchments (human-influenced (top) and natural (bottom) series) in disturbed period.

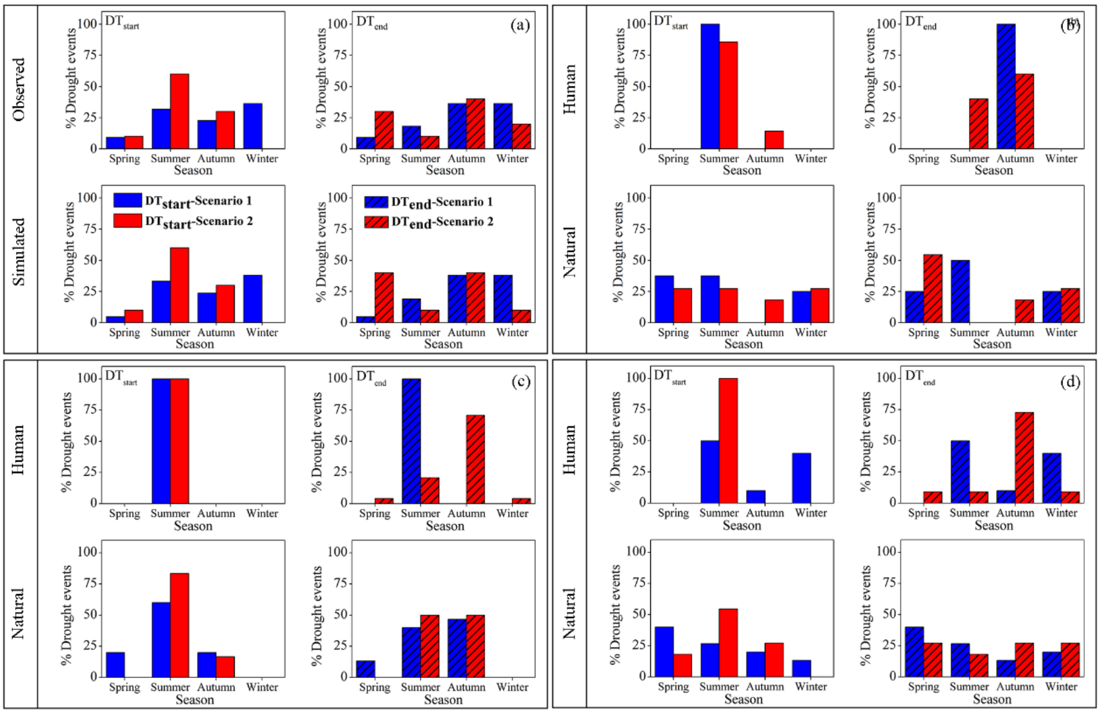

Fig. 11. Comparison of human influence on drought termination time of scenario 1 (D_{dur} < 3.43 months) and scenario 2 (D_{dur} > 3.43 months) in (a) Xiquan (observed (top) and simulated (bottom) series), (b) Xiaochengzi, (c) Dianzi, and (d) Taipingzhuang catchments (human-influenced (top) and natural (bottom) series) during disturbed period.

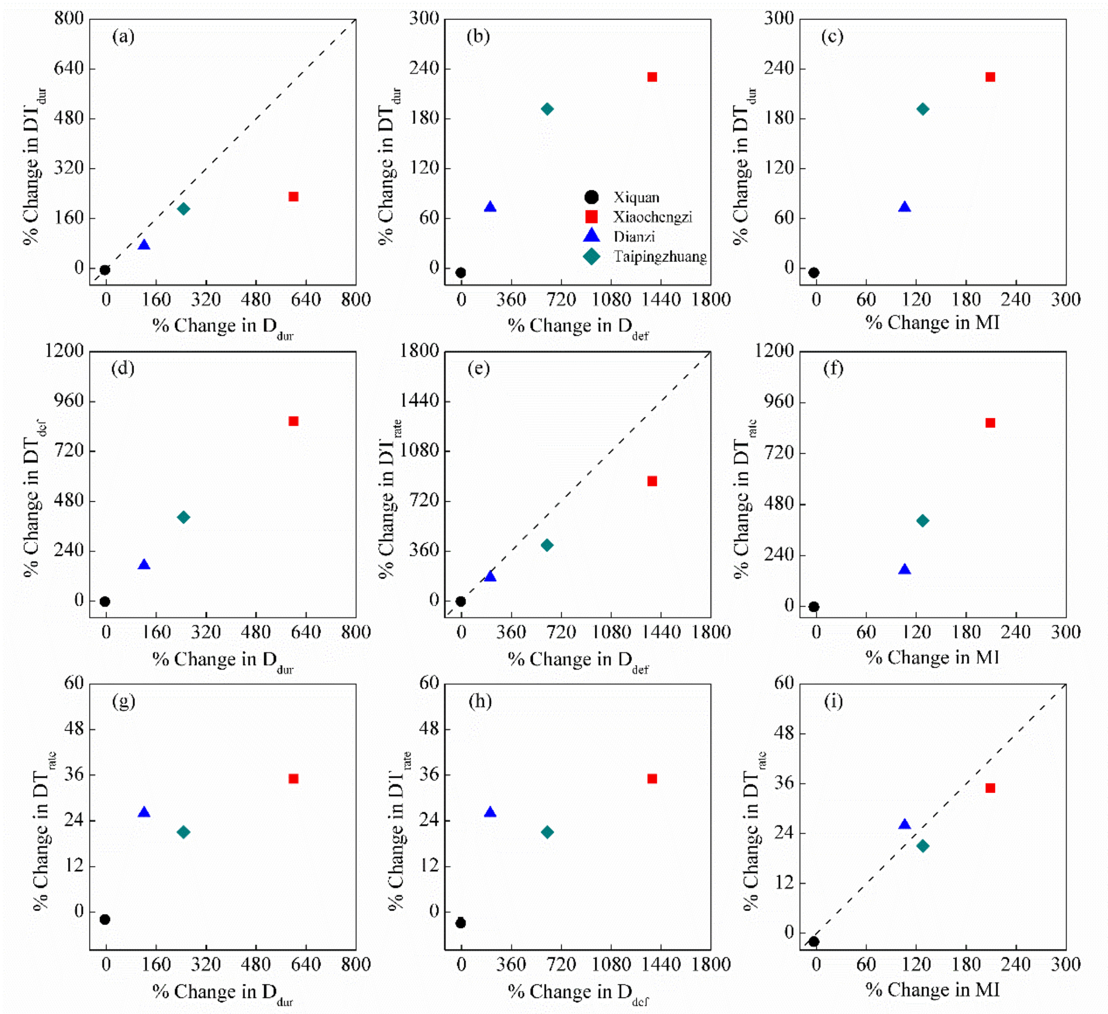

Fig. 12. Relationships between changes in drought characteristics and those in drought termination characteristics.

Table 1

Basic information about the four study catchments.

Hydrological station	Area (km^2)	Lon (E°)	Lat (N°)	Mean annual precipitation (mm)	Mean annual streamflow (mm)	Data period
Xiquan	419	118.53	41.42	572.88	126.45	1964–2016
Xiaochengzi	866	119.00	41.75	450.57	36.05	1964–2016
Dianzi	1643	118.83	41.42	523.26	63.43	1964–2016
Taipingzhuang	7720	119.25	42.20	438.53	26.57	1964–2016

Table 2

Results of MK trend analyses and Pettitt change-point tests of annual precipitation, potential evapotranspiration (PET), and streamflow for the four selected catchments for the period 1964–2016.

Hydrological station	MK trend test (year)						Pettitt test for change-point (year)		
	Precipitation		PET		Streamflow		Precipitation	PET	Streamflow
	Z value	Trend	Z value	Trend	Z value	Trend			
Xiquan	–1.57	↓	–1.20	↓	–0.41	↓	—	—	—
Xiaochengzi	–0.77	↓	–0.18	↓	**–4.18****	↓	—	—	1998**
Dianzi	–0.58	↓	–0.21	↓	**–2.48***	↓	—	—	1979**
Taipingzhuang	–0.58	↓	0.31	↑	**–5.07****	↓	—	—	1979**

Notes: ‘↓’ and ‘↑’ indicate downward and upward trends, respectively. ‘*’ and ‘**’ denote significance at 95% and 99% confidence levels, respectively.

Table 3

Physical meanings and numerical ranges of the seven parameters commonly calibrated in the VIC model.

Parameter	Physical meaning	Unit	Numerical range
B	Infiltration curve parameter	N/A	0−0.4
d_1	Thickness of top thin soil moisture layer	m	0.05−0.1
d_2	Thickness of middle soil moisture layer	m	0−2
d_3	Thickness of lower soil moisture layer	m	0−2
D_s	Fraction of D_{smax} where nonlinear baseflow begins	Fraction	0−1
D_{smax}	Maximum velocity of baseflow	mm/day	0−30
W_s	Fraction of maximum soil moisture where nonlinear baseflow occurs	Fraction	0−1

Table 4

Performance of streamflow (mm/month) simulation for the four catchments using the VIC model.

Catchment/Period	Calibration period				Validation period				Disturbed (simulation) period			
	NSE	LogNSE	BIAS (%)	CC	NSE	LogNSE	BIAS (%)	CC	NSE	LogNSE	BIAS (%)	CC
Xiquan	0.78	0.77	9.19	0.91	0.79	0.85	–5.8	0.92	0.77	0.86	–0.14	0.88
Xiaozchengzi	0.73	0.75	1.14	0.90	0.87	0.74	2.36	0.95	—	—	—	—
Dianzi	0.81	0.77	1.81	0.94	0.73	0.75	7.27	0.92	—	—	—	—
Taipingzhuang	0.90	0.72	5.00	0.95	0.82	0.80	5.47	0.91	—	—	—	—

Table 5

Differences in drought and drought termination characteristics between observed and simulated series in undisturbed period.

Case study	Differences in drought characteristics (%)				Differences in drought termination characteristics (%)		
	Drought frequency (D_{freq})	Mean drought duration (D_{dur})	Mean drought deficit (D_{def})	Mean maximum intensity (MI)	Mean termination duration (DT_{dur})	Mean termination deficit (DT_{def})	Mean termination rate (DT_{rate})
Xiquan	+3.6	+3.23	+0.50	+2.85	+4.76	–5.39	+2.65
Xiaochengzi	+6.90	+4.61	+3.44	+1.63	+3.57	+2.82	+1.83
Dianzi	+10.00	+0.65	–0.85	+1.96	+1.01	+3.05	+4.80
Taipingzhuang	+8.33	–2.26	+6.96	+7.13	–7.69	+7.20	+1.19
Mean value	+7.21	+1.55	+2.51	+3.39	+0.41	+1.92	+2.62

Table 6

Drought and drought termination characteristics of natural (simulated) series in disturbed period.

Case study	Predominant human activity	Natural drought characteristics				Natural drought termination characteristics		
		Drought frequency (D_{freq})	Mean drought duration (D_{dur}) (months)	Mean drought deficit (D_{def}) (mm)	Mean maximum intensity (MI) (mm)	Mean termination duration (DT_{dur}) (months)	Mean termination deficit (DT_{def}) (mm)	Mean termination rate (DT_{rate}) (mm/month)
Xiquan	——	31	3.61	13.11	6.17	2.68	10.11	2.78
Xiaochengzi	Human water withdrawal	19	3.89	3.86	2.37	2.12	2.78	1.56
Dianzi	Reservoir regulations, Human water withdrawal	21	3.00	9.43	5.51	1.90	7.52	3.34
Taipingzhuang	Land use change, Human water withdrawal	26	3.45	2.91	1.70	2.41	2.24	0.88

Table 7

Drought and drought termination characteristics of human-influenced series in disturbed period.

Case study	Predominant human activity	Human-influenced drought characteristics				Human-influenced drought termination characteristics		
		Drought frequency (D_{freq})	Mean drought duration (D_{dur}) (months)	Mean drought deficit (D_{def}) (mm)	Mean maximum intensity (MI) (mm)	Mean termination duration (DT_{dur}) (months)	Mean termination deficit (DT_{def}) (mm)	Mean termination rate (DT_{rate}) (mm/month)
Xiquan	——	32	3.47	12.70	6.00	2.53	9.80	2.73
Xiaochengzi	Human water withdrawal	7	27.29	56.90	7.33	7.00	26.78	2.11
Dianzi	Reservoir regulations, Human water withdrawal	27	6.63	29.03	11.36	3.30	20.34	4.22
Taipingzhuang	Land use change, Human water withdrawal	25	12.00	20.91	3.88	7.04	11.29	1.07

Table 8

Drought and drought termination characteristics of natural and human-influenced series for scenario 1 (D_{dur} < 3.43 months) and scenario 2 (D_{dur} > 3.43 months) during disturbed period.

Catchment	Scenario	Series	Drought characteristics				Drought termination characteristics		
			Drought frequency (D_{freq})	Mean drought duration (D_{dur}) (months)	Mean drought deficit (D_{def}) (mm)	Mean maximum intensity (MI) (mm)	Mean termination duration (DT_{dur}) (months)	Mean termination deficit (DT_{def}) (mm)	Mean termination rate (DT_{rate}) (mm/month)
Dianzi	Scenario 1	Natural	15	2.33	6.63	4.23	1.73	5.43	2.80
		Human-influenced	3	2.33	4.34	3.42	1.33	3.45	3.01
	Scenario 2	Natural	6	4.67	16.44	8.73	2.33	12.74	4.68
		Human-influenced	24	7.17	31.89	12.24	3.46	19.99	5.36
Taipingzhuang	Scenario 1	Natural	15	2.27	1.82	1.26	1.53	1.30	1.04
		Human-influenced	10	2.50	1.75	1.26	1.60	1.31	1.22
	Scenario 2	Natural	11	5.09	4.78	2.39	3.45	3.70	0.84
		Human-influenced	11	13.64	25.50	5.79	8.36	14.76	1.18

Table 9

Quantifying human influence on drought and drought termination characteristics in disturbed period.

Case study	Predominant human activity	Changes in drought characteristics (%)				Changes in drought termination characteristics (%)		
		Drought frequency (D_{freq})	Mean drought duration (D_{dur})	Mean drought deficit (D_{def})	Mean maximum intensity (MI)	Mean termination duration (DT_{dur})	Mean termination deficit (DT_{def})	Mean termination rate (DT_{rate})
Xiquan	——	+3	–4	–3	–3	–5	–3	–2
Xiaochengzi	Human water withdrawal	–63	**+601**	**+1376**	**+209**	**+230**	**+865**	**+35**
Dianzi	Reservoir regulations, Human water withdrawal	+29	+121	+208	+106	+73	+170	+26
Taipingzhuang	Land use change, Human water withdrawal	–15	+248	+619	+128	+192	+404	+21

Credit Author Statement

Wang Menghao: Conceptualization, Methodology, Software. Jiang Shanhu: Conceptualization, Project administration. Ren Liliang: Funding acquisition. Xu Chong-Yu: Writing-Review & Editing. Yuan Fei: Methodology. Liu Yi: Methodology. Yang Xiaoli: Methodology.

Declaration of Interest Statement

The author(s) declared no potential conflicts of interest with respect to the research, authorship, and publication of this article.

Figure
Click here to download high resolution image

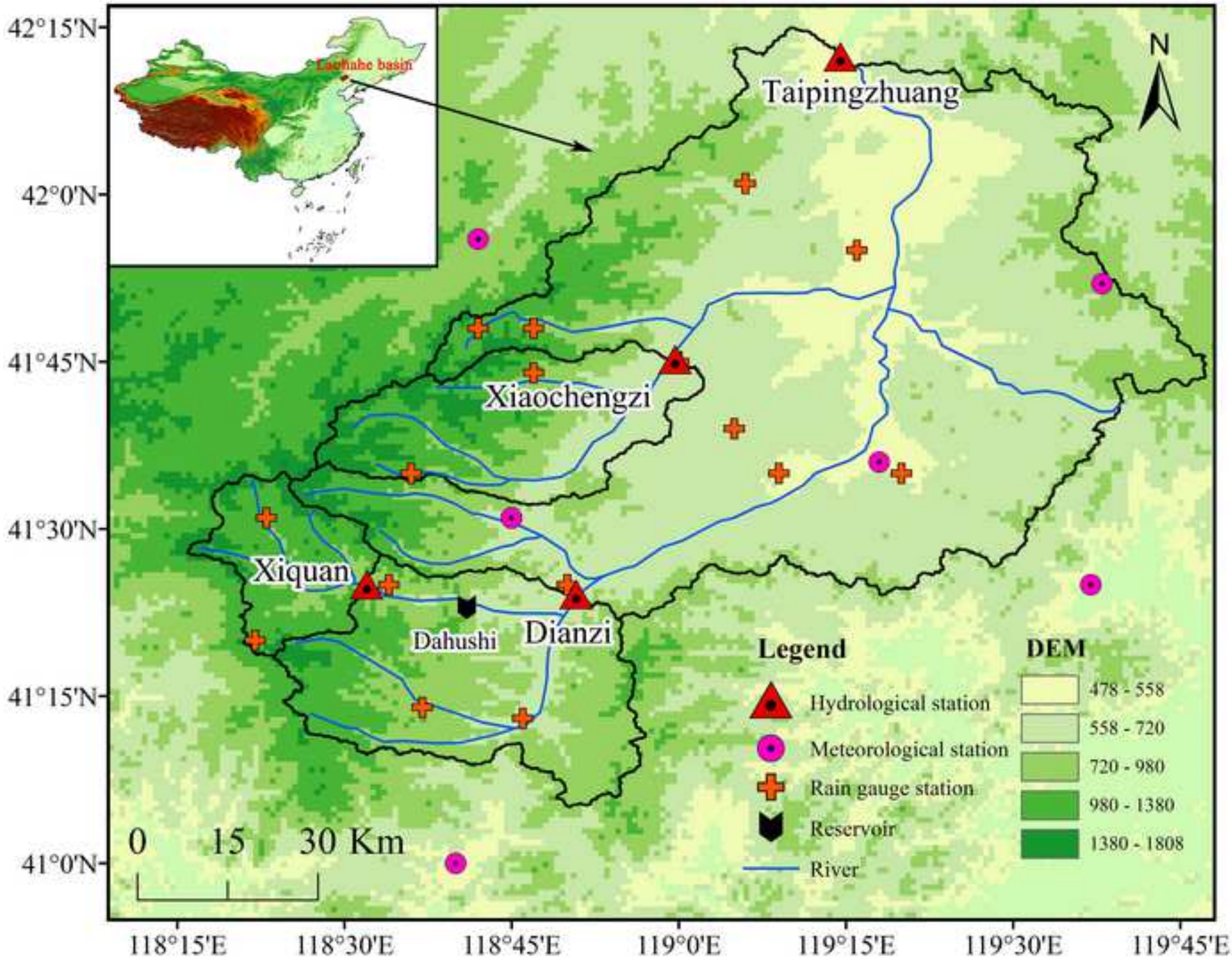

Figure
Click here to download high resolution image

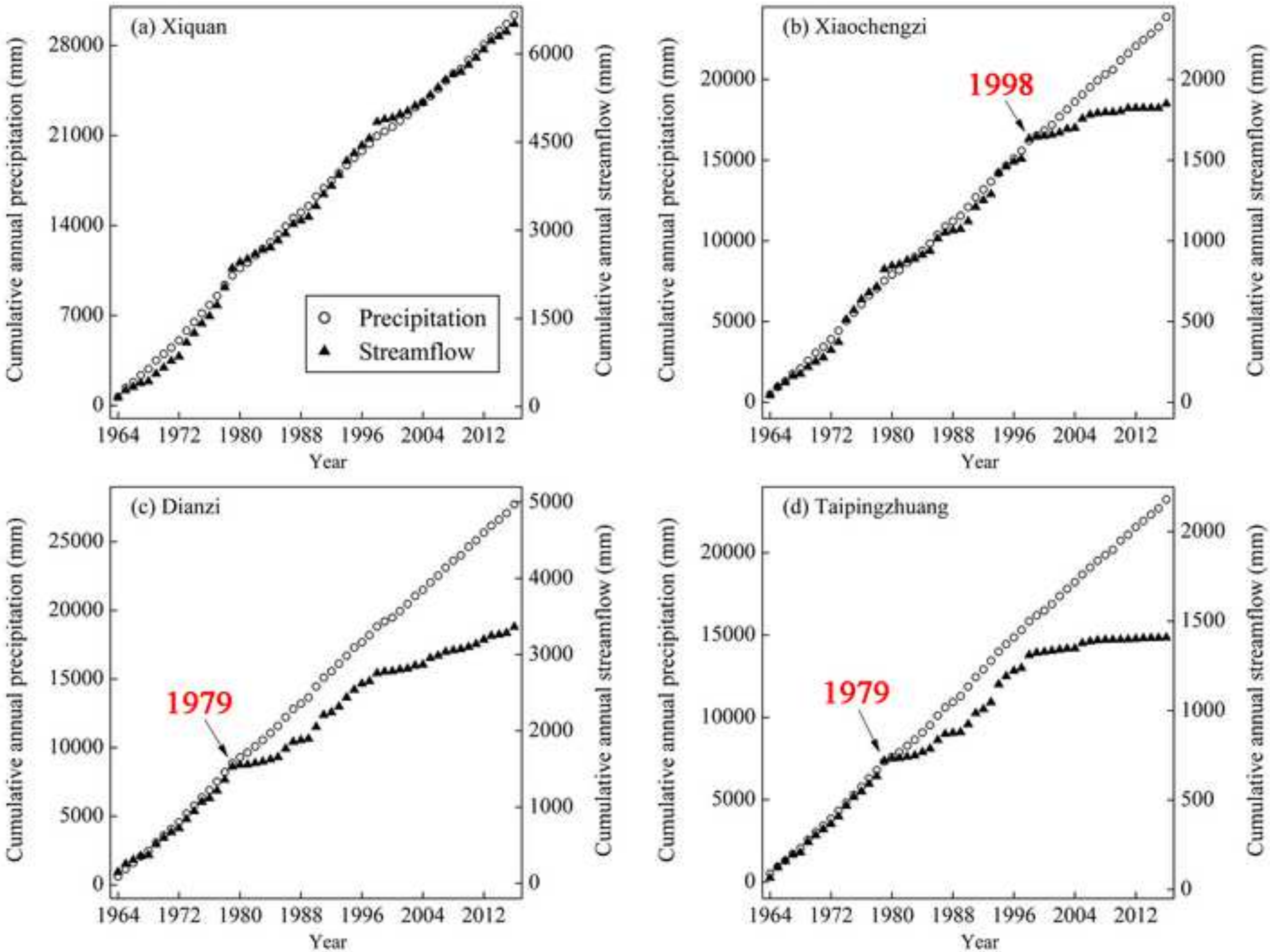

Figure
Click here to download high resolution image

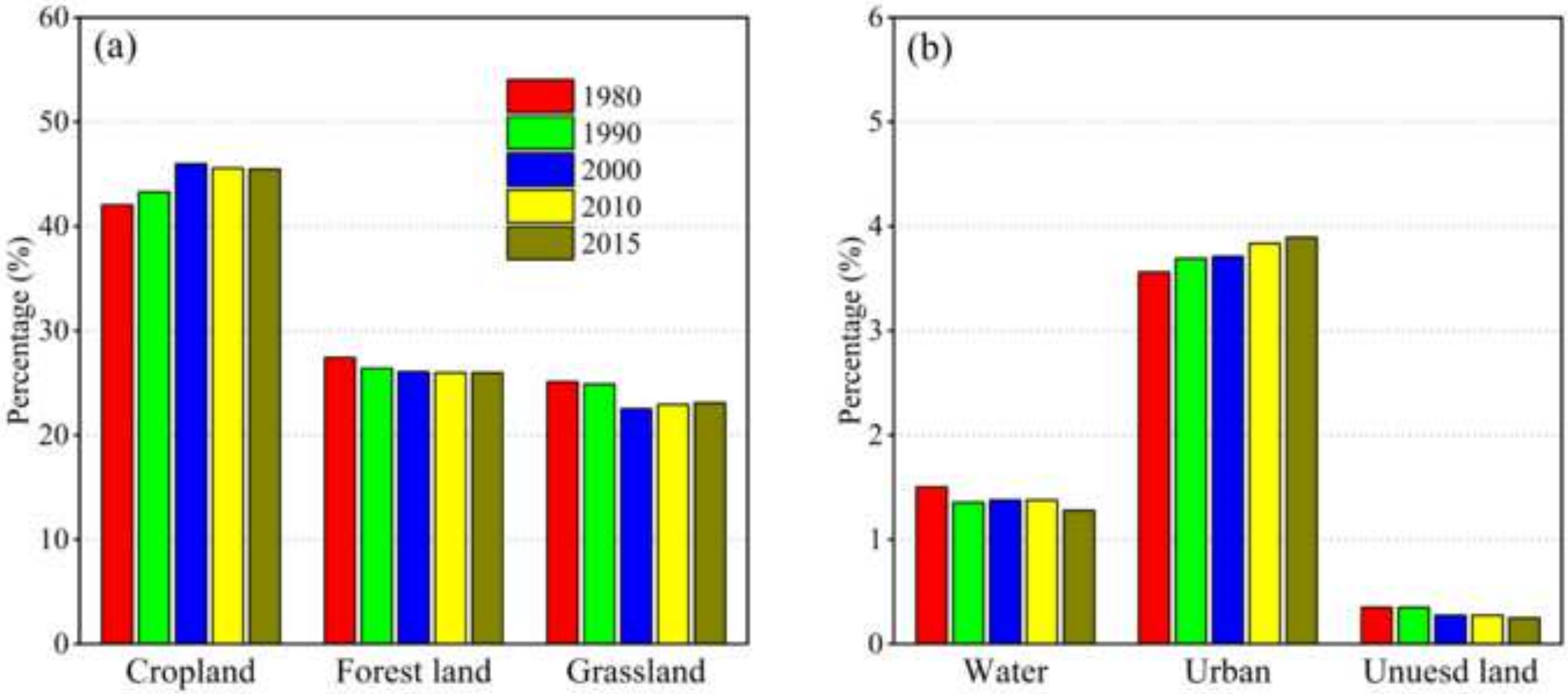

Figure
Click here to download high resolution image

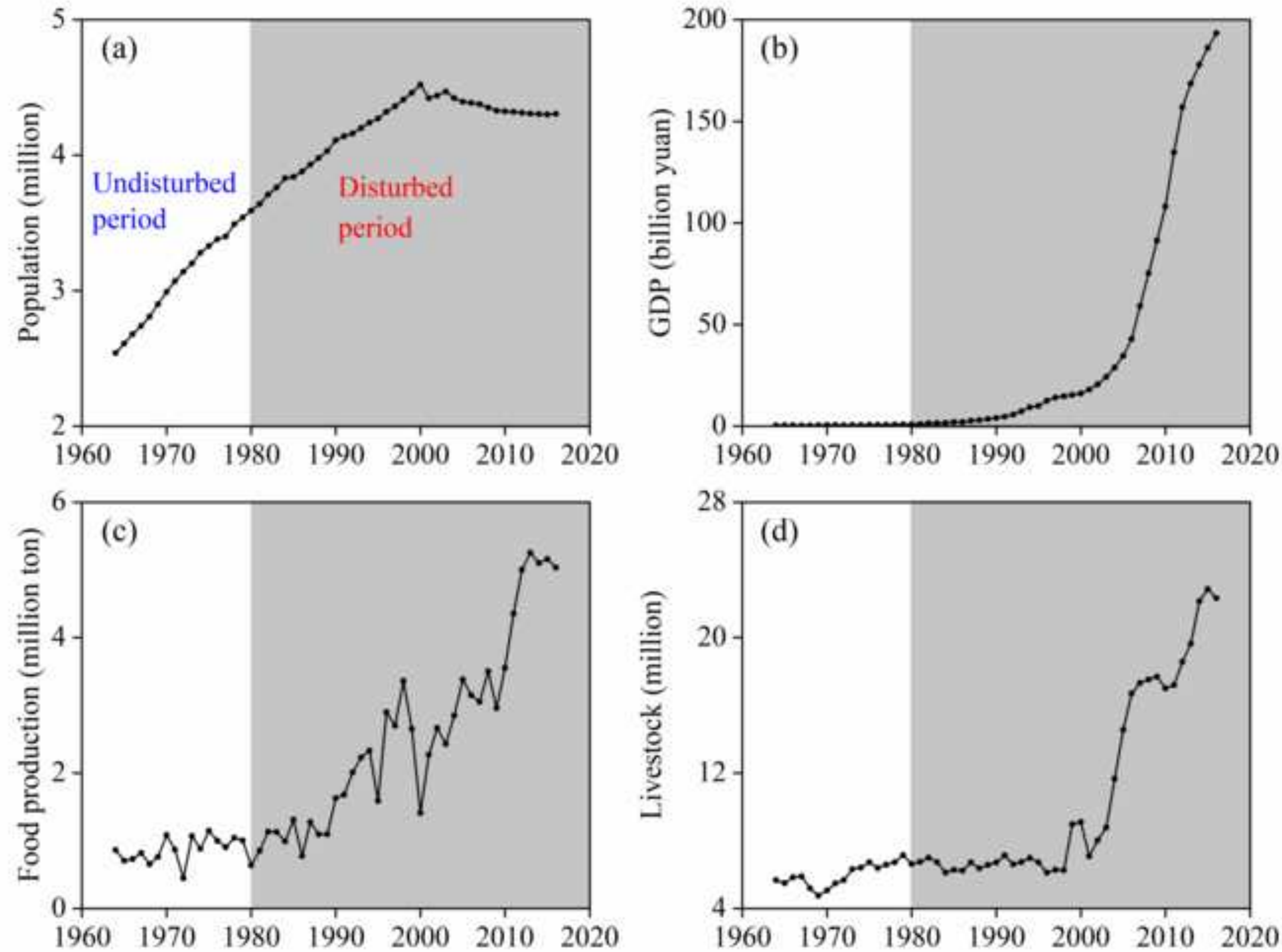

Figure

Click here to download high resolution image

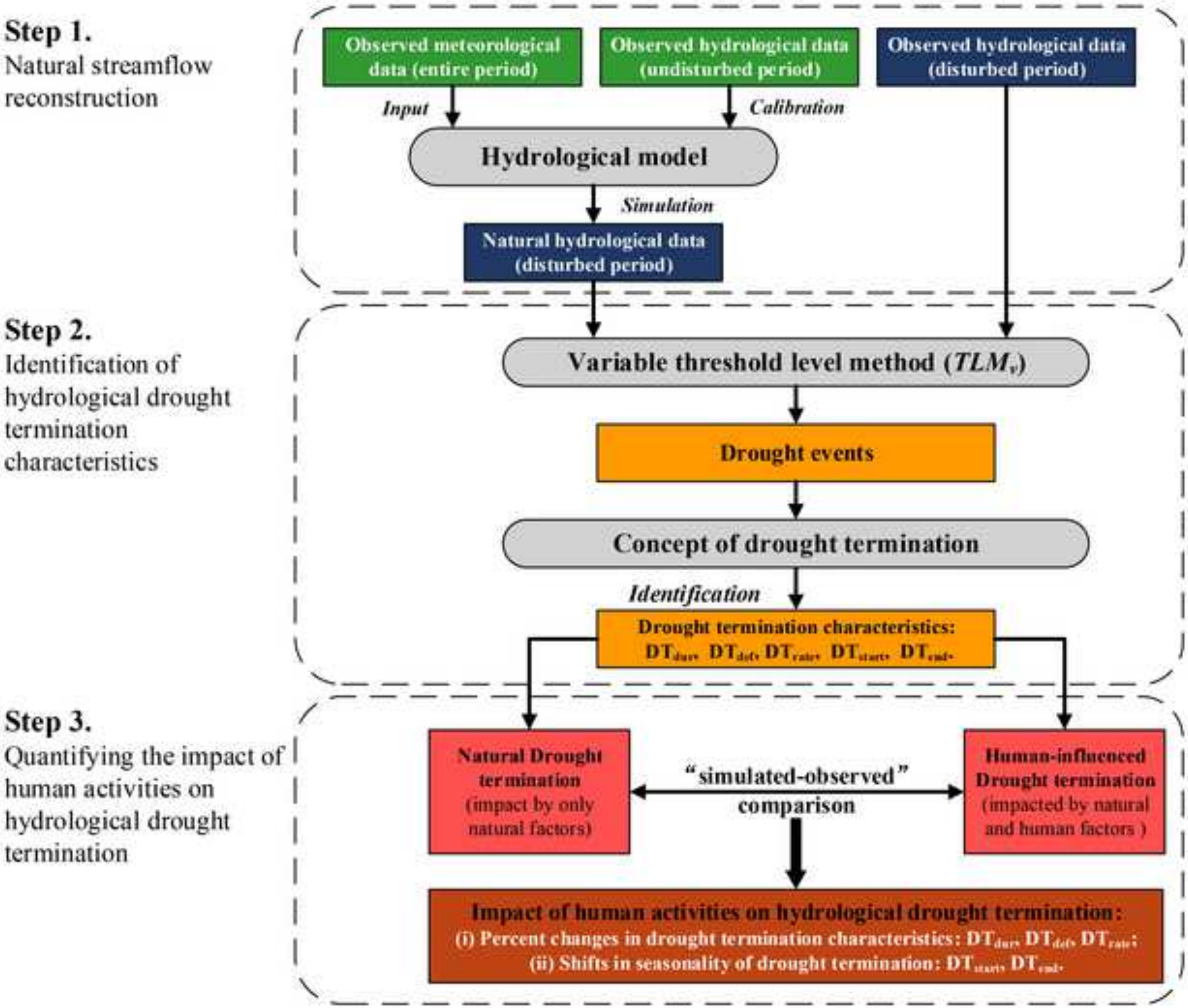

Figure

Click here to download high resolution image

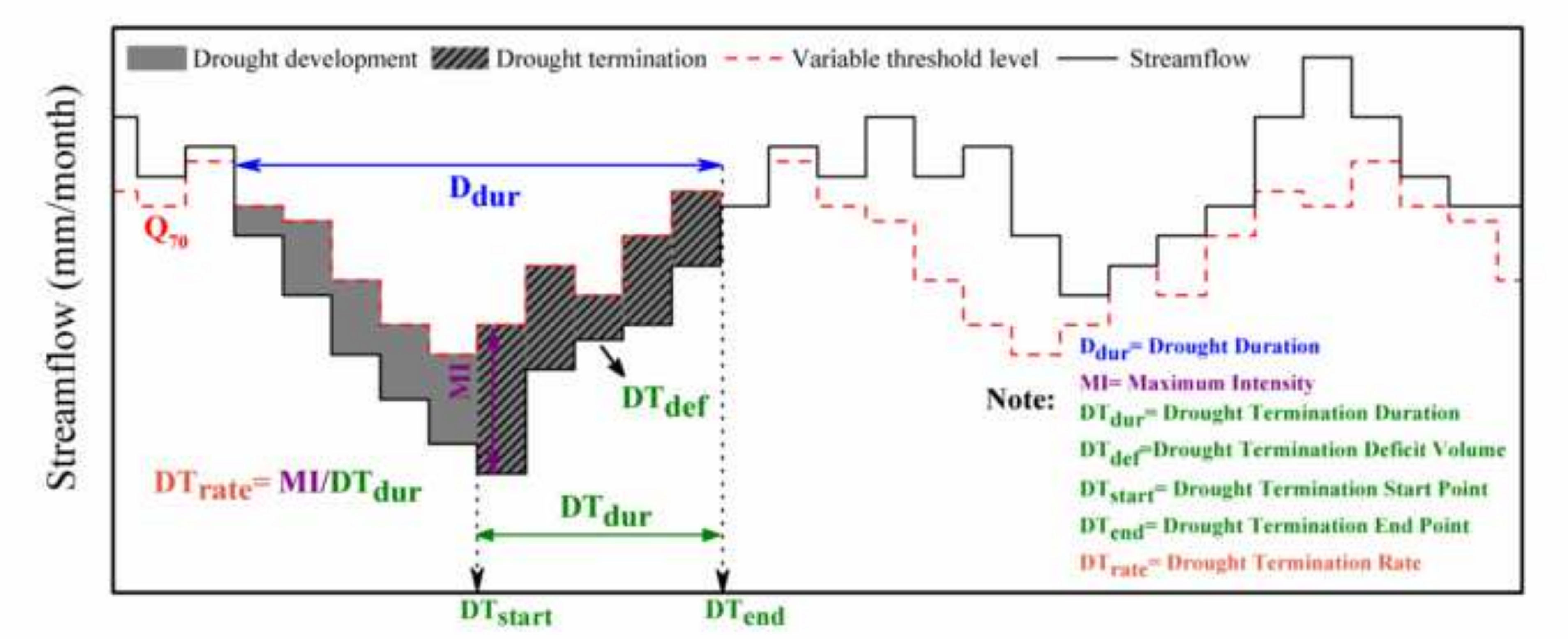

Figure

Click here to download high resolution image

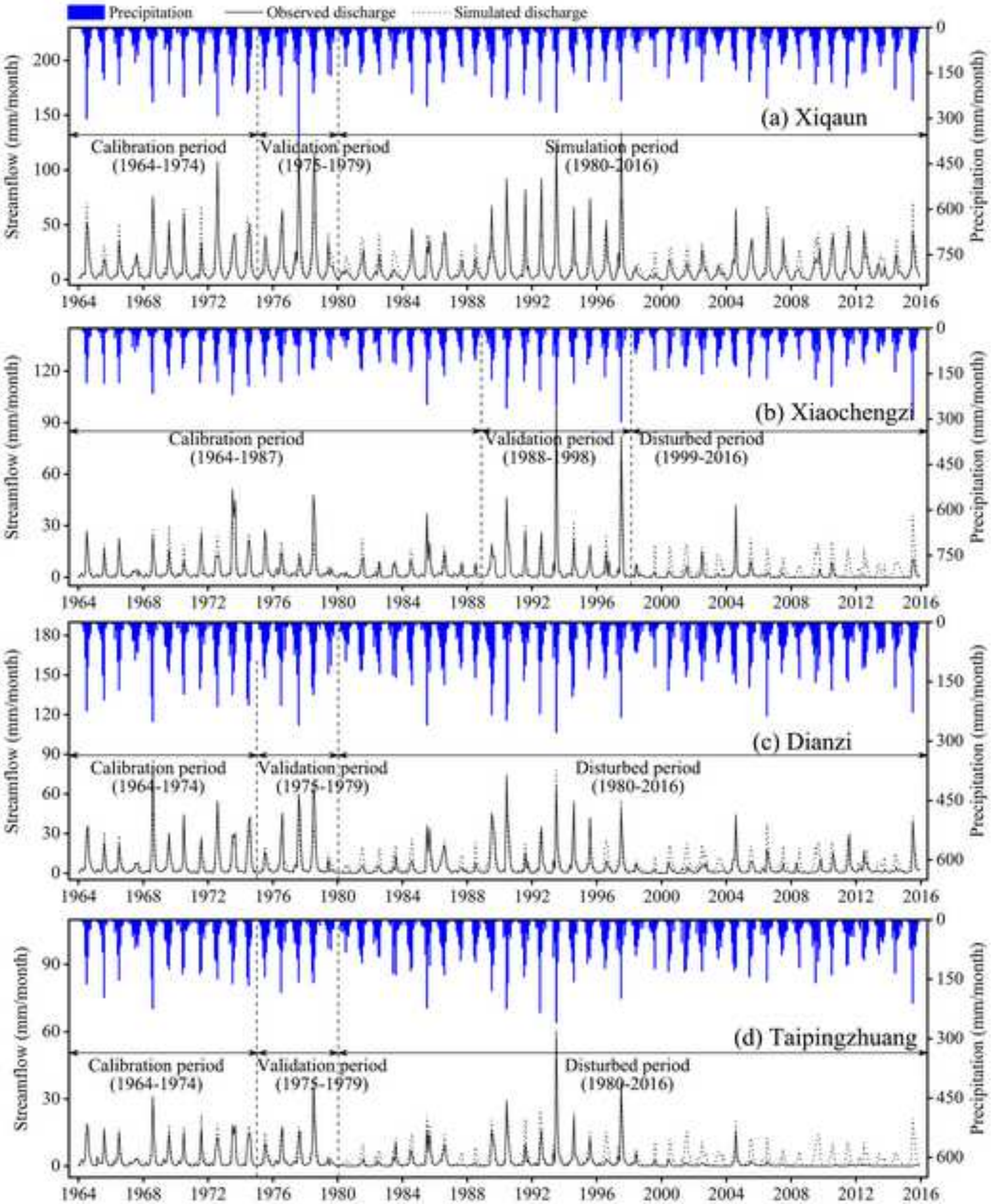

Figure

[Click here to download high resolution image]

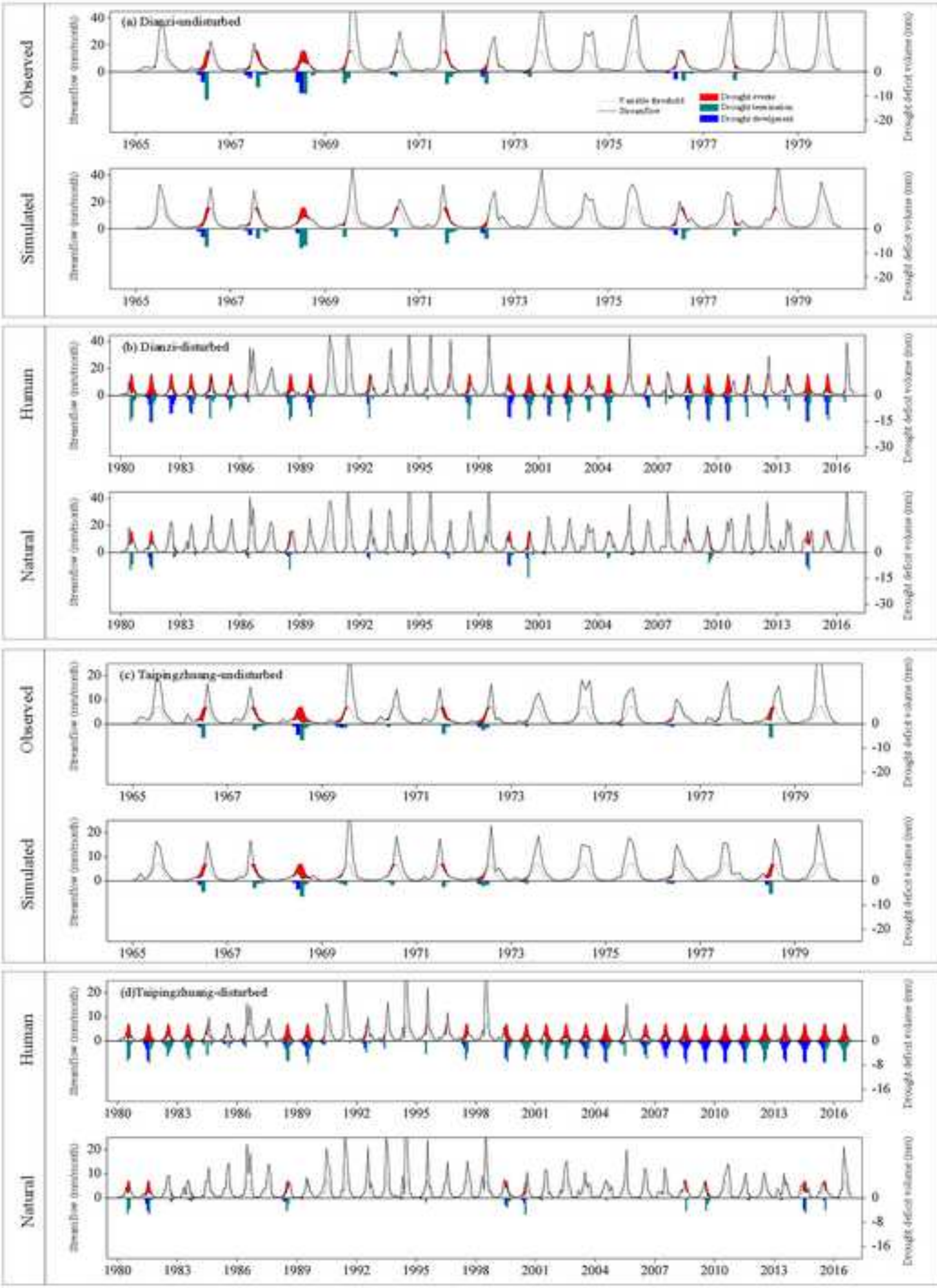

Figure

Click here to download high resolution image

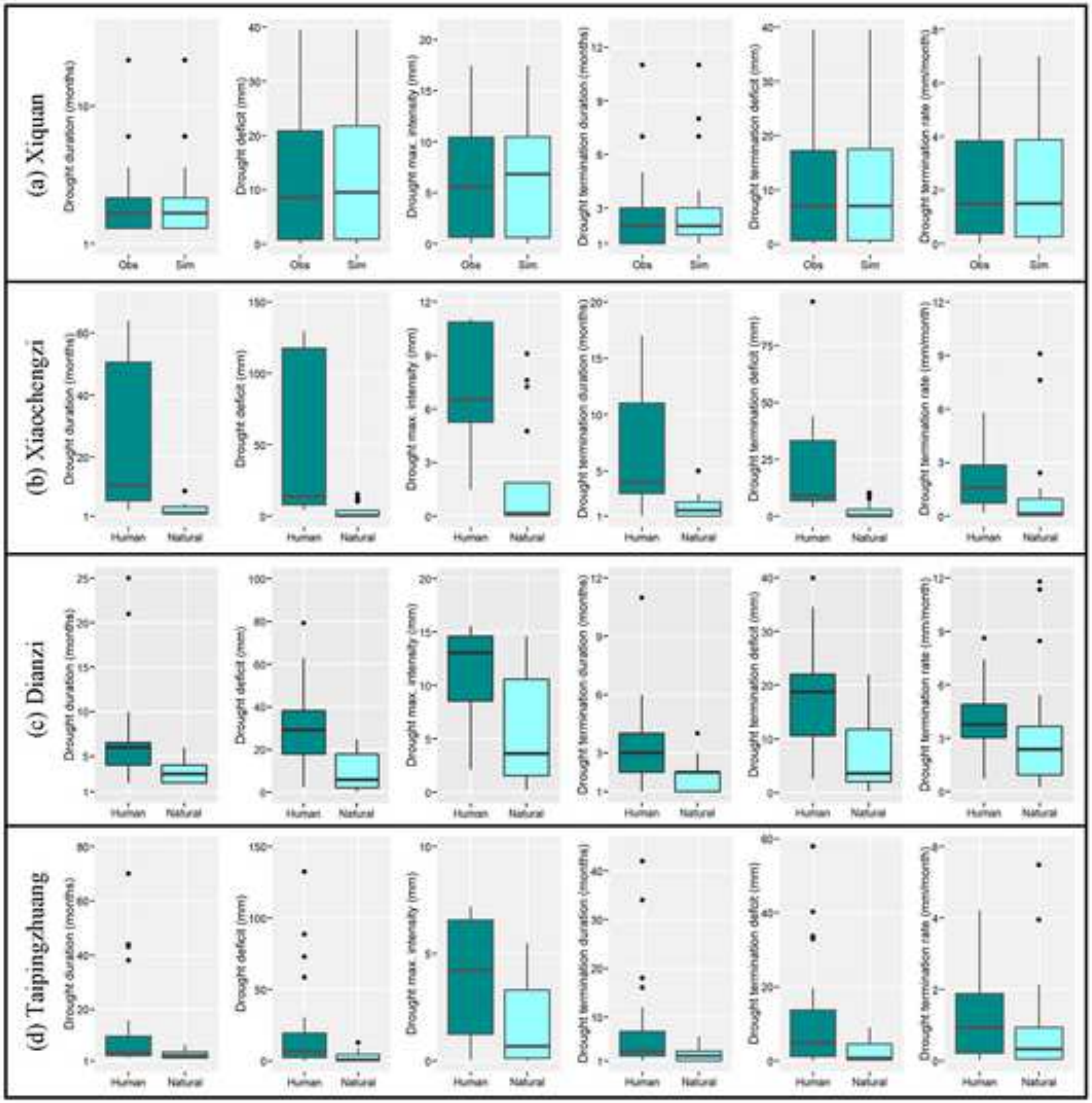

Figure
Click here to download high resolution image

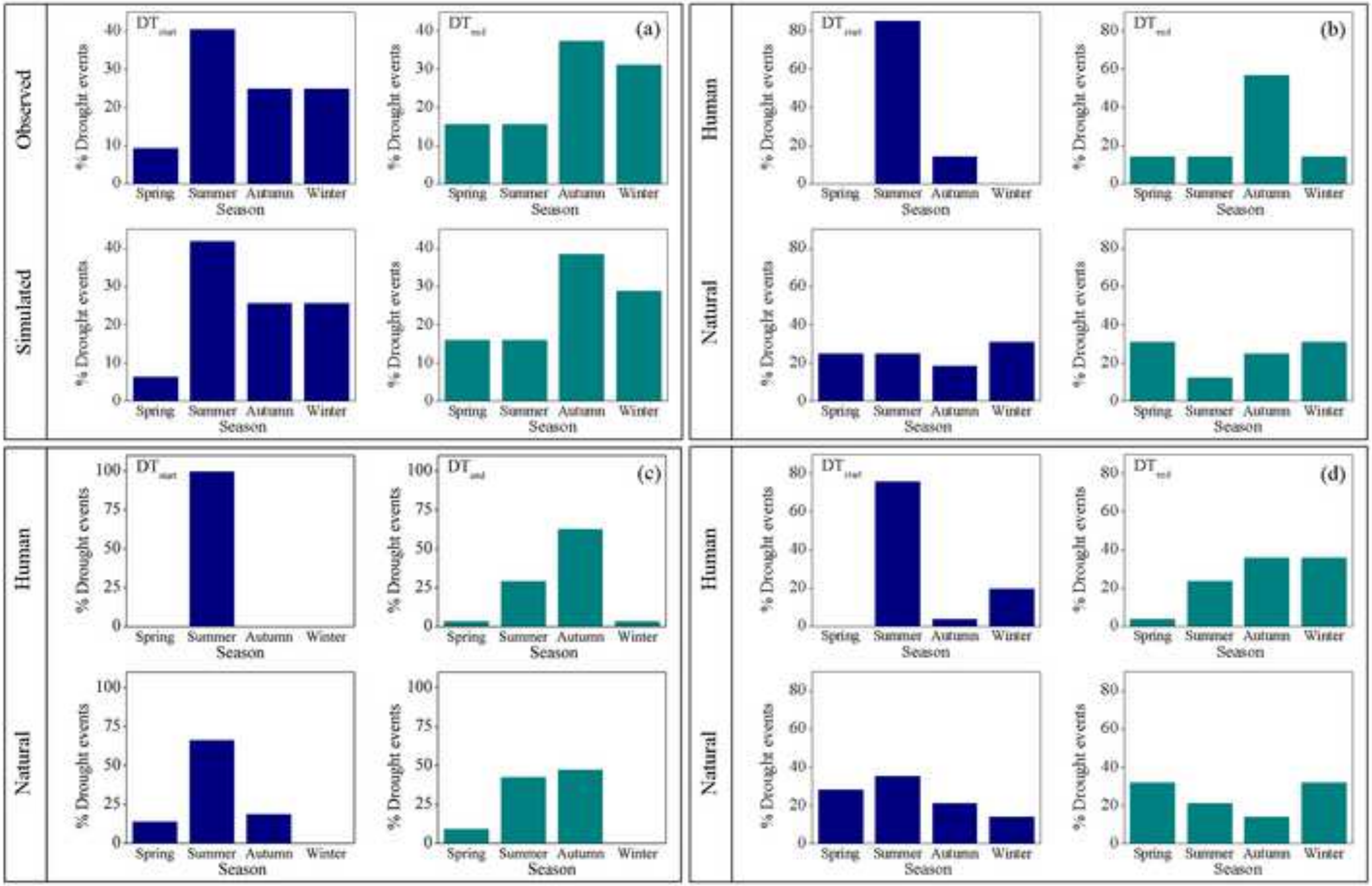

Figure
Click here to download high resolution image

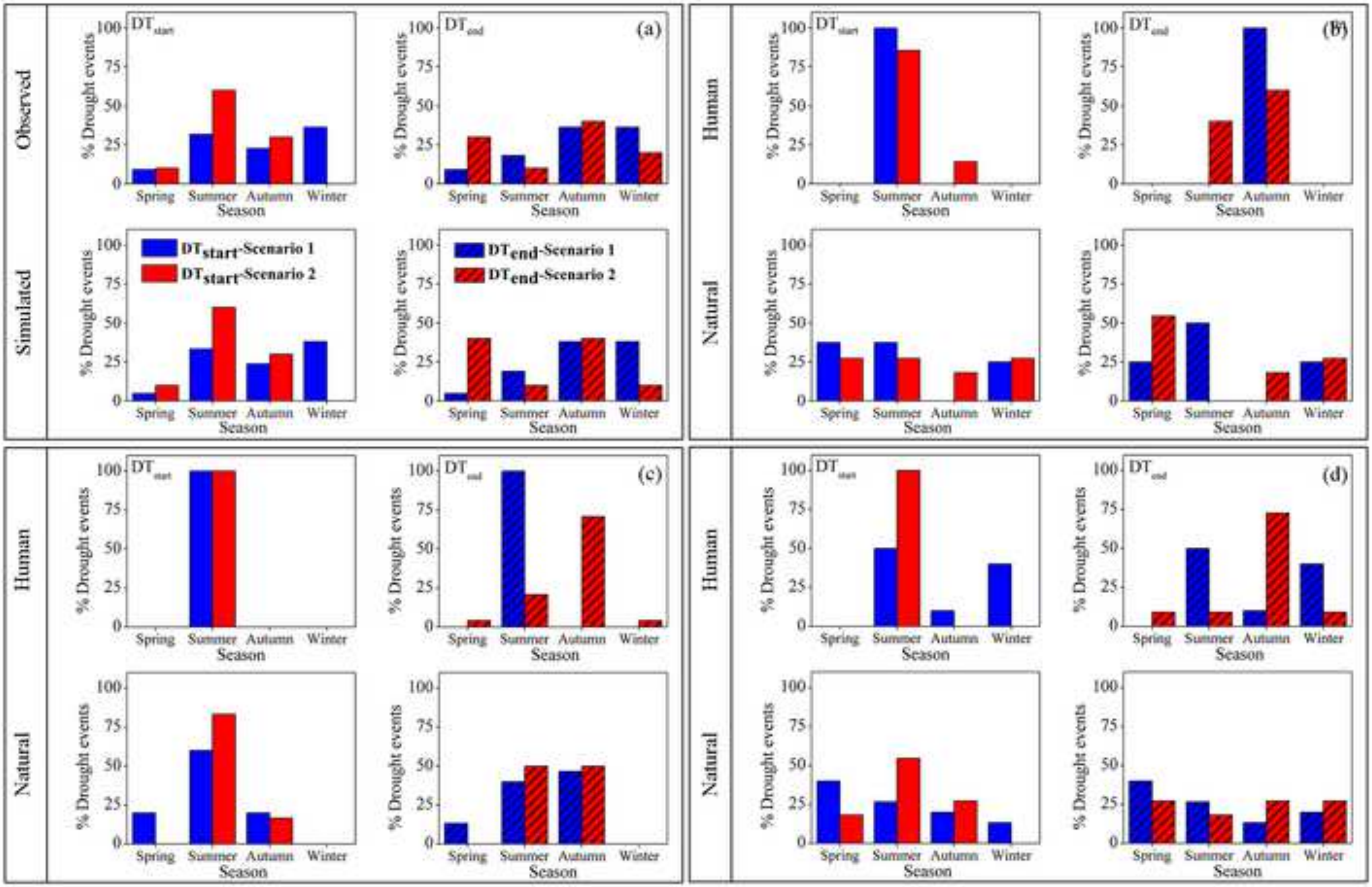

Figure

Click here to download high resolution image

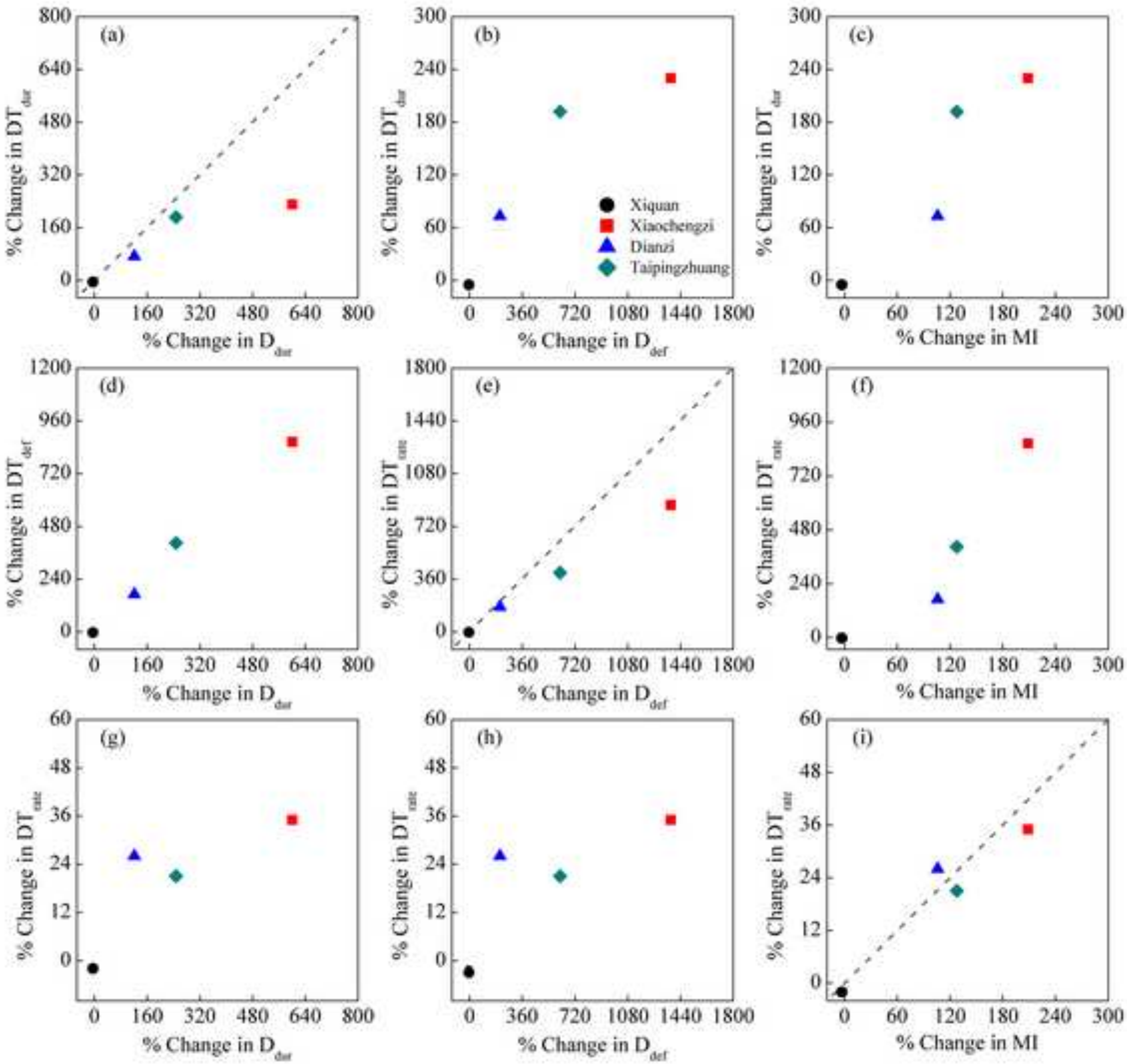

Table 1

Basic information about the four study catchments.

Hydrological station	Area (km^2)	Lon (E°)	Lat (N°)	Mean annual precipitation (mm)	Mean annual streamflow (mm)	Data period
Xiquan	419	118.53	41.42	572.88	126.45	1964–2016
Xiaochengzi	866	119.00	41.75	450.57	36.05	1964–2016
Dianzi	1643	118.83	41.42	523.26	63.43	1964–2016
Taipingzhuang	7720	119.25	42.20	438.53	26.57	1964–2016

Table 2

Results of MK trend analyses and Pettitt change-point tests of annual precipitation, potential evapotranspiration (PET), and streamflow for the four selected catchments for the period 1964–2016.

Hydrological station	MK trend test (year)						Pettitt test for change-point (year)		
	Precipitation		PET		Streamflow		Precipitation	PET	Streamflow
	Z value	Trend	Z value	Trend	Z value	Trend			
Xiquan	–1.57	↓	–1.20	↓	–0.41	↓	—	—	—
Xiaochengzi	–0.77	↓	–0.18	↓	**–4.18****	↓	—	—	1998**
Dianzi	–0.58	↓	–0.21	↓	**–2.48***	↓	—	—	1979**
Taipingzhuang	–0.58	↓	0.31	↑	**–5.07****	↓	—	—	1979**

Notes: ‘↓’ and ‘↑’ indicate downward and upward trends, respectively. ‘*’ and ‘**’ denote significance at 95% and 99% confidence levels, respectively.

Table 3

Physical meanings and numerical ranges of the seven parameters commonly calibrated in the VIC model.

Parameter	Physical meaning	Unit	Numerical range
B	Infiltration curve parameter	N/A	0−0.4
d_1	Thickness of top thin soil moisture layer	m	0.05−0.1
d_2	Thickness of middle soil moisture layer	m	0−2
d_3	Thickness of lower soil moisture layer	m	0−2
D_s	Fraction of D_{smax} where nonlinear baseflow begins	Fraction	0−1
D_{smax}	Maximum velocity of baseflow	mm/day	0−30
W_s	Fraction of maximum soil moisture where nonlinear baseflow occurs	Fraction	0−1

Table 4

Performance of streamflow (mm/month) simulation for the four catchments using the VIC model.

Catchment/Period	Calibration period				Validation period				Disturbed (simulation) period			
	NSE	LogNSE	BIAS (%)	CC	NSE	LogNSE	BIAS (%)	CC	NSE	LogNSE	BIAS (%)	CC
Xiquan	0.78	0.77	9.19	0.91	0.79	0.85	–5.8	0.92	0.77	0.86	–0.14	0.88
Xiaozchengzi	0.73	0.75	1.14	0.90	0.87	0.74	2.36	0.95	—	—	—	—
Dianzi	0.81	0.77	1.81	0.94	0.73	0.75	7.27	0.92	—	—	—	—
Taipingzhuang	0.90	0.72	5.00	0.95	0.82	0.80	5.47	0.91	—	—	—	—

Table 5

Differences in drought and drought termination characteristics between observed and simulated series in undisturbed period.

Case study	Differences in drought characteristics (%)				Differences in drought termination characteristics (%)		
	Drought frequency (D_{freq})	Mean drought duration (D_{dur})	Mean drought deficit (D_{def})	Mean maximum intensity (MI)	Mean termination duration (DT_{dur})	Mean termination deficit (DT_{def})	Mean termination rate (DT_{rate})
Xiquan	+3.6	+3.23	+0.50	+2.85	+4.76	− 5.39	+2.65
Xiaochengzi	+6.90	+4.61	+3.44	+1.63	+3.57	+2.82	+1.83
Dianzi	+10.00	+0.65	–0.85	+1.96	+1.01	+3.05	+4.80
Taipingzhuang	+8.33	–2.26	+6.96	+7.13	–7.69	+7.20	+1.19
Mean value	+7.21	+1.55	+2.51	+3.39	+0.41	+1.92	+2.62

Table 6

Drought and drought termination characteristics of natural (simulated) series in disturbed period.

Case study	Predominant human activity	Natural drought characteristics				Natural drought termination characteristics		
		Drought frequency (D_{freq})	Mean drought duration (D_{dur}) (months)	Mean drought deficit (D_{def}) (mm)	Mean maximum intensity (MI) (mm)	Mean termination duration (DT_{dur}) (months)	Mean termination deficit (DT_{def}) (mm)	Mean termination rate (DT_{rate}) (mm/month)
Xiquan	——	31	3.61	13.11	6.17	2.68	10.11	2.78
Xiaochengzi	Human water withdrawal	19	3.89	3.86	2.37	2.12	2.78	1.56
Dianzi	Reservoir regulations, Human water withdrawal	21	3.00	9.43	5.51	1.90	7.52	3.34
Taipingzhuang	Land use change, Human water withdrawal	26	3.45	2.91	1.70	2.41	2.24	0.88

Table 7

Drought and drought termination characteristics of human-influenced series in disturbed period.

Case study	Predominant human activity	Human-influenced drought characteristics				Human-influenced drought termination characteristics		
		Drought frequency (D_{freq})	Mean drought duration (D_{dur}) (months)	Mean drought deficit (D_{def}) (mm)	Mean maximum intensity (MI) (mm)	Mean termination duration (DT_{dur}) (months)	Mean termination deficit (DT_{def}) (mm)	Mean termination rate (DT_{rate}) (mm/month)
Xiquan	——	32	3.47	12.70	6.00	2.53	9.80	2.73
Xiaochengzi	Human water withdrawal	7	27.29	56.90	7.33	7.00	26.78	2.11
Dianzi	Reservoir regulations, Human water withdrawal	27	6.63	29.03	11.36	3.30	20.34	4.22
Taipingzhuang	Land use change, Human water withdrawal	25	12.00	20.91	3.88	7.04	11.29	1.07

Table 8

Drought and drought termination characteristics of natural and human-influenced series for scenario 1 (D_{dur} < 3.43 months) and scenario 2 (D_{dur} > 3.43 months) during disturbed period.

Catchment	Scenario	Series	Drought characteristics				Drought termination characteristics		
			Drought frequency (D_{freq})	Mean drought duration (D_{dur}) (months)	Mean drought deficit (D_{def}) (mm)	Mean maximum intensity (MI) (mm)	Mean termination duration (DT_{dur}) (months)	Mean termination deficit (DT_{def}) (mm)	Mean termination rate (DT_{rate}) (mm/month)
Dianzi	Scenario 1	Natural	15	2.33	6.63	4.23	1.73	5.43	2.80
		Human-influenced	3	2.33	4.34	3.42	1.33	3.45	3.01
	Scenario 2	Natural	6	4.67	16.44	8.73	2.33	12.74	4.68
		Human-influenced	24	7.17	31.89	12.24	3.46	19.99	5.36
Taipingzhuang	Scenario 1	Natural	15	2.27	1.82	1.26	1.53	1.30	1.04
		Human-influenced	10	2.50	1.75	1.26	1.60	1.31	1.22
	Scenario 2	Natural	11	5.09	4.78	2.39	3.45	3.70	0.84
		Human-influenced	11	13.64	25.50	5.79	8.36	14.76	1.18

Table 9

Quantifying human influence on drought and drought termination characteristics in disturbed period.

Case study	Predominant human activity	Changes in drought characteristics (%)				Changes in drought termination characteristics (%)		
		Drought frequency (D_{freq})	Mean drought duration (D_{dur})	Mean drought deficit (D_{def})	Mean maximum intensity (MI)	Mean termination duration (DT_{dur})	Mean termination deficit (DT_{def})	Mean termination rate (DT_{rate})
Xiquan	——	+3	–4	–3	–3	–5	–3	–2
Xiaochengzi	Human water withdrawal	–63	**+601**	**+1376**	**+209**	**+230**	**+865**	**+35**
Dianzi	Reservoir regulations, Human water withdrawal	+29	+121	+208	+106	+73	+170	+26
Taipingzhuang	Land use change, Human water withdrawal	–15	+248	+619	+128	+192	+404	+21

Figure captions

Fig. 1. Location of the study areas and distribution of the hydrological, meteorological, and rain gauge stations.

Fig. 2. Double cumulative curves of annual precipitation and streamflow in (a) Xiquan, (b) Xiaochengzi, (c) Dianzi, and (d) Taipingzhuang catchments.

Fig. 3. Land use changes for the study area in the disturbed period: (a) Cropland, Forest land, and Grassland and (b) Water, Urban, and Unused land.

Fig. 4. Changes of socioeconomic data for the study area during 1964–2016 (undisturbed period and disturbed period): (a) population, (b) GDP, (c) food population, and (d) number of livestock.

Fig. 5. Proposed approach for identifying hydrological drought termination characteristics and quantifying the impact of human activities on hydrological drought termination.

Fig. 6. Definition of drought termination (modified from Parry et al., 2016; Margariti et al., 2019)

Fig. 7. Comparisons of VIC-simulated and observed monthly streamflow for Xiquan (undisturbed and simulation periods), Xiaochengzi, Dianzi, and Taipingzhuang catchments (undisturbed and disturbed periods).

Fig. 8. Identification and comparison of drought termination characteristics for observed and simulated series during undisturbed period, and for human-influenced and natural series during disturbed period in Dianzi and Taipingzhuang catchments.

Fig. 9. Boxplots of drought and those of drought termination characteristics for (a) Xiquan (observed (left) and simulated (right) series), (b) Xiaochengzi, (c) Dianzi, and (d) Taipingzhuang catchments (human-influenced (left) and natural (right) series).

Fig. 10. Changes of seasonality of drought termination starting and ending for (a) Xiquan (observed (top) and simulated (bottom) series), (b) Xiaochengzi, (c) Dianzi, and (d) Taipingzhuang catchments (human-influenced (top) and natural (bottom) series) in disturbed period.

Fig. 11. Comparison of human influence on drought termination time of scenario 1 (D_{dur} < 3.43 months) and scenario 2 (D_{dur} > 3.43 months) in (a) Xiquan (observed (top) and simulated (bottom) series), (b) Xiaochengzi, (c) Dianzi, and (d) Taipingzhuang catchments (human-influenced (top) and natural (bottom) series) during disturbed period.

Fig. 12. Relationships between changes in drought characteristics and those in drought termination characteristics.